

EXPERIMENTAL DEVELOPMENT OF A
SHORT FLEXIBLE PLATE NOZZLE
USING THE INFLUENCE METHOD

Thesis by

Danny Frederick Huebner

In Partial Fulfillment of the Requirement

For the Degree of

Aeronautical Engineer

California Institute of Technology

Pasadena, California

1958

ACKNOWLEDGEMENTS

The author wishes to express his sincere appreciation to Dr. Clark B. Millikan for his interest and valuable comments during this investigation. He is also indebted to Mr. Edwin Pounder for his extensive advice and to the members of the CWT Aerodynamics Department staff for their work in the preparation of the figures. Thanks are also in order to Mrs. Elizabeth Fox for her unequalled typing ability displayed herein.

ABSTRACT

The purpose of this investigation was to determine the possibility of using a semi-empirical technique, the Influence Method, to shorten the CWT supersonic flexible plate nozzle. The experiments were conducted in the CWT $8\frac{1}{2}$ x 11 feet flexible plate nozzle at $M_{CAM} = 1.600$ and $M_{CAM} = 1.700$.

The Influence Method and its application to shortening a flexible plate nozzle are presented and discussed. Included are comparisons of the theoretical and experimental jack influence parameters. Theoretical length estimates are presented which determine to what extent the CWT nozzle could be shortened.

Results indicate that the Influence Method can be used to shorten the CWT supersonic flexible plate nozzle. The usable testing length was increased by approximately 35% at both the Mach numbers investigated. However, as the nozzle becomes shorter the undesirable Mach number variation, in the region occupied by models, increases from ± 0.005 to ± 0.015 .

TABLE OF CONTENTS

PART	TITLE	PAGE
	ACKNOWLEDGEMENTS	
	ABSTRACT	
	TABLE OF CONTENTS	
I	INTRODUCTION	1
II	THEORETICAL DEVELOPMENT OF THE INFLUENCE METHOD	
	A. INTRODUCTION	4
	B. FLOW DISTURBANCE FIELDS IN A FLEXIBLE PLATE NOZZLE	4
	C. THE JACK INFLUENCE FUNCTIONS	5
	D. THE CORRECTION EQUATIONS	6
III	THEORETICAL LIMITATIONS TO SHORTENING THE CWT FLEXIBLE PLATE NOZZLE	
	A. INTRODUCTION	8
	B. THE SHORTEST POSSIBLE THEORETICAL NOZZLE	9
	C. ESTIMATE OF NOZZLE LENGTHS	10
IV	EXPERIMENTAL PROCEDURE AND RESULTS	
	A. INTRODUCTION	13
	B. TEST PROCEDURE	13
	C. THE FUNDAMENTAL INFLUENCE METHOD PARAMETERS	13
	1. Jack Influence Curves	14
	2. Linearity Data	15
	3. Superposition Data	15
	D. SHORT NOZZLE DISTRIBUTIONS	16
V	CONCLUSIONS	19
	REFERENCES	21

TABLE OF CONTENTS (Cont'd)

PART	TITLE	PAGE
	APPENDIX I. NOTATION	
	A. Notation Used for the Influence Method	22
	B. Notation Used for the Theoretical Length Estimates	23
	C. Notation Used to Describe Configurations Tested	24
	APPENDIX II. RUN SCHEDULE	25
	APPENDIX III. LIST OF FIGURES	28
	FIGURES	30-53

I. INTRODUCTION

The purpose of a supersonic nozzle is to establish flow at the nozzle exit. This flow should be parallel to the nozzle centerline, uniform, and at a constant Mach number.

Normally nozzles for supersonic wind tunnels are two-dimensional. This requires controllable shapes on two of the walls, usually the floor and ceiling. The other two walls are flat and parallel.

To obtain the controllable shapes needed for the two movable walls, flexible plates mounted on jacks are used. This method is very useful in obtaining the required geometry. The flexible plates used to obtain various predetermined contours produce any given test section Mach number in the design Mach number range.

The Southern California Cooperative Wind Tunnel supersonic nozzle (Fig. 1) is of the flexible type. The floor and ceiling are composed of flexible plates supported on a series of jacks. The jacks are pin jointed to the plates at the axial stations shown in Fig. 1. The sidewalls are straight and parallel.

The nozzle thus formed is symmetrical about the tunnel centerline and is designed to produce test section Mach numbers in the range $1.00 \leq M_{CAM} \leq 1.80$. Flexible plate contours can be produced to establish the flow, but operation is limited by model size and wave reflection.

Model size is now limited, excluding wave reflection limitations, by the location of the leading edge of the test rhombus with respect to the nozzle exit. For the CWT supersonic nozzle this distance is a function of Mach number as shown in

Fig. 2. The usable testing length is reduced from 10.73 feet at $M_{CAM} = 1.30$ to 6.74 feet at $M_{CAM} = 1.70$. It should be noted that these lengths are the maximum available for the combination of the model and support system (i. e. sting).

It is desirable to develop a shorter nozzle which increases the distance between the leading edge of the test rhombus and nozzle station 21.0 feet. This is desirable especially at the higher Mach numbers. This analysis will investigate the possible experimental development of short nozzles at the CWT using the Influence Method. The investigation was done at $M_{CAM} = 1.600$ and $M_{CAM} = 1.700$ because the usable testing length is most severely limited at these two Mach numbers.

The Influence Method was originally developed for use in flexible plate nozzles (Refs. 1, 2 and 3). It is a method to minimize local axial variations in Mach number and flow angle in the region occupied by the models. Various combinations of jack deflections were determined which when applied minimized the undesirable variations in both Mach number and flow angle on the tunnel centerline.

In this analysis the Influence Method is modified for use in developing short nozzles and is applied specifically to the CWT supersonic nozzle for $M_{CAM} = 1.60$ and $M_{CAM} = 1.70$.

To orient the experimental results obtained, the shortest theoretical nozzles are calculated for $M_{CAM} = 1.60$ and $M_{CAM} = 1.70$. To attain these theoretical limits a method of approximating the lengths of various short nozzles had to be

found. The method developed by Riise (Ref. 4) is used. By various checks it was determined that this method results in calculated nozzle lengths accurate to within 1%. These data prescribe the region in which the Influence Method should be applied and offer criteria for interpreting the experimental results obtained.

II. THEORETICAL DEVELOPMENT OF THE INFLUENCE METHOD

A. INTRODUCTION

The Influence Method was originally developed, for use in flexible plate nozzles (Refs. 1, 2, and 3), as a means to minimize local axial variations in both Mach number and flow direction in the region occupied by models. This was accomplished by determining various combinations of jack deflections which, when applied, minimized the undesirable variations in Mach number and flow direction on the tunnel centerline.

In order to adapt this method to shortening a flexible plate nozzle we have to assume that there exists a centerline Mach number distribution which results in a shorter nozzle. We then utilize the Influence Method to determine the combination of jack deflections which will result in the nearest solution to the desired distribution.

The development of the Influence Method as applied to the flexible plate nozzle is presented with particular emphasis on adapting the method to enable a shorter nozzle to be developed experimentally at the CWT.

B. FLOW DISTURBANCE FIELDS IN A FLEXIBLE PLATE NOZZLE

In general a flexible plate nozzle will produce supersonic flow with two main disturbance fields, one from the flexible plates and one from the sidewalls. The usual problem is to make these disturbance fields as small as possible in the region occupied by models.

The two fields are experimentally measured together and a basic problem is to separate them using the data which are available. Assuming that this can be done reasonably well the next step is to investigate each field independently. This presentation will consider only the disturbances initiating from the flexible plates.

The disturbances from the nozzle plates in general will be three-dimensional because of non-uniformities in plate shape across the flow. However it seems logical to assume the field will be almost two-dimensional because of the manner in which the plates are bent. Also the disturbances should be small enough to add linearly. Hence one can assume that the disturbance field will behave according to characteristics theory.

The field in general can be defined in terms of Mach number and flow direction distributions in the region of interest. In particular if $\mathcal{E}_M(x)$ is defined as the difference between the desired and the existing Mach number distributions between a and b on the tunnel centerline the entire flow field can be defined within the Mach lines as shown in Fig. 3.

Because of symmetry $\mathcal{E}_M(x)$ can be corrected by a symmetric deflection of the plates about the centerline without affecting $\mathcal{E}_\theta(x)$, $\mathcal{E}_\theta(x)$ can be corrected by an antisymmetric deflection of the plates without affecting $\mathcal{E}_M(x)$. Hence a discussion of only $\mathcal{E}_M(x)$ is justified with the restriction that only symmetric deflections of the plate are used.

It should be emphasized however that the success of such a correction depends basically on how well the sidewall disturbances can be separated from $\mathcal{E}_M(x)$.

C. THE JACK INFLUENCE FUNCTIONS.

The corrections that can be made to the disturbance field must be accomplished by moving the plate jacks either with the trim controls or by reshaping the cams.

Theoretically (neglecting viscous and non-linear effects) along characteristics lines

$$\delta \theta_{w_{i,j}} = I_{\theta_{i,j}} \quad (1)$$

and at any point in the flow

$$|I_{\theta_{i,j}}| = \frac{d\theta}{dM} |I_{M_{i,j}}| \quad (2)$$

Basically in order to apply a correction the $I_{\theta}(x)$ and $I_M(x)$ functions have to be known for all the jacks that are going to be used and at all the Mach numbers that are considered. The following assumptions are made and must be verified experimentally:

1. $\prod \theta_i$ is linear with respect to $\Delta_{i,j}$ within desired range
2. I_{θ_i} and I_{θ_j} are symmetric
3. Equation 2 is valid

D. THE CORRECTION EQUATIONS

Once $\mathcal{E}_M(x)$, is determined and the required jack influence functions are measured experimentally the best settings for any given number of jacks to minimize $\mathcal{E}_M(x)$ in the region a - b can be determined by a least squares scheme. In setting up the scheme the following sign conventions are made: (See Fig. 4)

$$\begin{aligned} (\pm I_{\theta_i})(+\Delta_i) &= \pm \text{slope change on centerline} \\ (\pm I_{\theta_j})(+\Delta_j) &= \mp \text{slope change on centerline} \end{aligned}$$

which means that

$$I_{M_{i,j}} = \frac{1}{d\theta/dM} I_{\theta_{i,j}} \quad (3)$$

Hence the corrections for the symmetric function, $\mathcal{E}_M(x)$, can be set up as a set of simultaneous equations.

For this purpose let:

$$\Delta_{M_i} = \Delta_i = \Delta_j \quad i = j \quad \text{For } \mathcal{E}_M \text{ correction}$$

where Δ_{M_i} are the correcting jack settings determined by solving the simultaneous equations.

Let P be the number of jack stations to be used for the correction and K = (1, 2 --- P) be any jack station in this group. The P equations are then obtained as follows:

For the symmetrical $\mathcal{E}_M(x)$ corrections in the interval a - b

$$\int_a^b \mathcal{E}_M(x) \Pi_{M_K}(x) dx + \sum_{i=1}^P \left[\int_a^b \Pi_{M_i}(x) \Pi_{M_K}(x) dx \right] \Delta_{M_i} = 0 \quad (4)$$

written out for P = 4 (4 jack stations used for correction) these equations appear as:

$$\begin{aligned} \Delta_{M_1} \int_a^b \Pi_{M_1}^2 dx + \Delta_{M_2} \int_a^b \Pi_{M_1} \Pi_{M_2} dx + \Delta_{M_3} \int_a^b \Pi_{M_1} \Pi_{M_3} dx + \Delta_{M_4} \int_a^b \Pi_{M_1} \Pi_{M_4} dx &= - \int_a^b \mathcal{E}_M \Pi_{M_1} dx \\ \Delta_{M_1} \int_a^b \Pi_{M_2} \Pi_{M_1} dx + \Delta_{M_2} \int_a^b \Pi_{M_2}^2 dx + \Delta_{M_3} \int_a^b \Pi_{M_2} \Pi_{M_3} dx + \Delta_{M_4} \int_a^b \Pi_{M_2} \Pi_{M_4} dx &= - \int_a^b \mathcal{E}_M \Pi_{M_2} dx \\ \Delta_{M_1} \int_a^b \Pi_{M_3} \Pi_{M_1} dx + \Delta_{M_2} \int_a^b \Pi_{M_3} \Pi_{M_2} dx + \Delta_{M_3} \int_a^b \Pi_{M_3}^2 dx + \Delta_{M_4} \int_a^b \Pi_{M_3} \Pi_{M_4} dx &= - \int_a^b \mathcal{E}_M \Pi_{M_3} dx \\ \Delta_{M_1} \int_a^b \Pi_{M_4} \Pi_{M_1} dx + \Delta_{M_2} \int_a^b \Pi_{M_4} \Pi_{M_2} dx + \Delta_{M_3} \int_a^b \Pi_{M_4} \Pi_{M_3} dx + \Delta_{M_4} \int_a^b \Pi_{M_4}^2 dx &= - \int_a^b \mathcal{E}_M \Pi_{M_4} dx \end{aligned} \quad (5)$$

Where Δ_{M_i} are the unknowns and Π_{M_i} , Π_{M_K} and \mathcal{E}_M are determined from experimental data.

III. THEORETICAL LIMITATIONS TO SHORTENING THE CWT FLEXIBLE PLATE NOZZLE

A. INTRODUCTION

The present CWT flexible plate nozzle has parallel sidewalls with the floor and ceiling each supported by ten jacks pin-jointed to the nozzle plate. The jack spacing is 2.5 feet with the exception that jacks 1 and 2 are 2.0 feet apart. Fig. 1 presents the geometric dimensions of the modified CWT flexible plate nozzle.

The present CWT nozzle family is composed of modified Foelsch nozzles. As is commonly known Foelsch nozzles combine source flow up to the inflection point and plane wave flow downstream of the inflection point with the characteristic discontinuity in curvature at the inflection point itself. Because of this discontinuity at the inflection point it is impossible for a pin-jointed plate to duplicate the desired contour, hence one has to apply the boundary condition that the curvature at the inflection point has to be zero. An additional boundary condition is applied at the inflection point, i. e. the curvature slope be continuous, to enable the pin-supported plate to approximate more closely the theoretical nozzle contour (Ref. 4). The application of these boundary conditions results in a partial cancellation region immediately downstream of the inflection point. A schematic is shown in Fig. 5.

B. THE SHORTEST POSSIBLE THEORETICAL NOZZLE

The shortest possible flexible plate nozzle is theoretically obtained when $\theta_{IP}/\theta_i \approx 1.0$ (no partial cancellation region) and $\theta_i/\psi_i \approx 1.0$. However from a practical standpoint neither of these limits can be obtained. The $\theta_{IP}/\theta_i \approx 1.0$ limit cannot be obtained

with a flexible plate nozzle as the actual plate shape cannot match the theoretically required nozzle contour. Hence this limit is structural. The $\theta_i/\alpha_i = 1.0$ limit cannot be reached from a practical standpoint because of an aerodynamic limit which, in the form of compression waves, becomes a problem as $\theta_i/\alpha_i \rightarrow 1.0$.

The present CWT flexible plate nozzle was designed to maintain a continuous third derivative (continuous curvature slope) at the inflection point and $\theta_{IP}/\theta_i = 0.50$ was assumed for $1.300 \leq M \leq 1.800$. From characteristics theory the relation defining the nozzle family is:

$$v_i = v_e - \frac{\theta_i}{2} \quad 3 - \frac{\theta_{IP}}{\theta_i} \quad (6)$$

and to keep compression waves from occurring (i.e. overexpanded nozzle)

$$\frac{\theta_i}{v_i} = \frac{2K}{5-3K} \leq 1$$

where

$$K = \frac{5\theta_i}{2v_e + \theta_{IP}}$$

The additional boundary condition that the third derivative at the inflection point be continuous requires that in addition to Eq. 6 the following relation must also be satisfied.

$$\frac{\theta_i \tan^3 \theta_i}{(\alpha_i \sin \theta_i - \theta_i)^2} = \frac{9}{16} \frac{\tan^2 \mu_i}{(1 - \theta_{IP}/\theta_i)} \alpha_i^2 \quad (7)$$

Hence Eqs. 6 and 7 are the defining relations for the general CWT nozzle family, and M_e , θ_{IP} , and θ_i are the three parameters which completely define a particular nozzle in the family.

In order to shorten the present nozzle three cases have theoretically been considered, namely:

- 1) Maintain the third derivative continuous condition and increase both θ_{1P}/θ_i and θ_i/ν_i according to Eqs. 6 and 7. θ_i/ν_i will reach the theoretical limit of one first.
- 2) Relaxing the third derivative continuous feature and maintaining the present value of θ_{1P}/θ_i (equal to 0.5 for the present family) increase θ_i/ν_i to the theoretical limit of one according to Eq. 6.
- 3) Relaxing the third derivative feature and maintaining the present value of θ_i/ν_i (function of Mach number) increase θ_{1P}/θ_i to the theoretical limit of one according to Eq. 6.

C. ESTIMATE OF NOZZLE LENGTHS

Each of the three cases was then investigated to determine how short a nozzle could be made as the theoretical limits were approached. The method developed by Riise (Ref. 4) for determining the approximate length of a flexible plate nozzle was used and a brief discussion of this method follows.

This method divides the nozzle into four parts, namely X_1 , ΔX_1 , ΔX_2 , and ΔX_3 . Referring to Fig. 6 X_1 is computed from the initial curve equations by the relation:

$$X_1 = \frac{X_i - X_t}{H/2} = \frac{3}{2} \frac{\cot \theta_i}{\tau_i} \left(\frac{\tau_i \sin \theta_i - 1}{\theta_i} \right) \quad (8)$$

ΔX_3 is a known function of Mach number, namely,

$$\frac{\Delta X_3}{H/2} = \frac{X_e - X_G}{H/2} = \sqrt{M_e^2 - 1} \quad (9)$$

Hence the approximate length of a given nozzle involves the estimation of ΔX_1 , and ΔX_2 . ΔX_1 and ΔX_2 are estimated by the following relations:

$$\frac{\Delta X_1}{H/2} = \frac{X_{WP} - X_i}{H/2} = \left\{ \left[\frac{y_i (\theta_i - \theta_{IP}) / \theta_i}{\sin [(\mu_{IPWP} + \theta_{IPWP}) - \theta_{LWP}]} \right] \left[\sin [90 - (\mu_{IPWP} + \theta_{IPWP})] \right] \right\} \frac{\cos \theta_{LWP}}{H/2} \quad (10)$$

$$\frac{\Delta X_2}{H/2} = \frac{X_G - X_{WP}}{H/2} = \frac{\left\{ \left[\frac{y_i (\theta_i - \theta_{IP}) / \theta_i}{\sin [(\mu_{IPWP} + \theta_{IPWP}) - \theta_{LWP}]} \right] \left[\sin [90 - (\mu_{IPWP} + \theta_{IPWP})] \right] \right\} \sin \theta_{LWP} + y_i}{H/2 \tan (\mu_{WPG} - \theta_{WPG})}$$

where

$$\begin{aligned} \theta_{WPG} &= \frac{\theta_{WP} + \theta_G}{2} \\ \theta_{IPWP} &= \frac{\theta_{IP} + \theta_{WP}}{2} \\ \theta_{LWP} &= \frac{\theta_i + \theta_{WP}}{2} \\ y_i &= H/2 \frac{z_i}{z_e} \frac{\sin \theta_i}{\theta_i} \end{aligned}$$

$$\mu_{WPG} = \text{func.} \left(\frac{V_{WP} + V_G}{2} \right)$$
$$\mu_{IPWP} = \text{func.} \left(\frac{V_{IP} + V_{WP}}{2} \right)$$

Utilizing this method it was found that the length of the present CWT flexible plate nozzle, which was computed using characteristics theory, could be estimated within 1%. Another check of this method is readily available as the theoretical limit of case three is a Foelsch nozzle. The approximate method, in the limit, reduces to the exact solution for the length of a Foelsch nozzle.

The theoretical estimates were then calculated for various nozzles in each of the three cases and are presented in Figs. 7 and 8. The increments of shortened length, with respect to the present CWT flexible plate nozzle, are presented in Figs. 9, 10, and 11. The nozzle plate stress limit now in use is included on these plots. This limit represents 45% of the yield stress and was exceeded during the experimental phase of this study.

IV. EXPERIMENTAL PROCEDURE AND RESULTS

A. INTRODUCTION

The experimental phase of this investigation consisted of two parts: 1) the confirmation of the fundamental parameters used in the Influence Method, and 2) the short nozzle distributions obtained when the Influence Method was applied to the CWT nozzle.

An explanation of the test procedure will be presented first followed by a discussion of the two experimental phases.

B. TEST PROCEDURE

Static pressure measurements were obtained using the CWT 3" probe (CWT Drwg. 4280). This probe contains 75 orifices which enable measurements every two inches from station 6.97 feet to station 21.46 feet inclusive. The pressure leads from the 3" probe were connected to a multiple manometer bank filled with acetylene tetrabromide. / At each desired condition a 35 mm. picture was taken of the multiple manometer bank and the resulting data were reduced by the standard CWT film reading procedure. This procedure results in the pressure coefficient $\frac{P_o - P_x}{P_o}$. These pressure coefficients were then converted to M_x (the local Mach number) using the Electrodata Datatron.

C. THE FUNDAMENTAL INFLUENCE METHOD PARAMETERS

The fundamental parameters which were investigated experimentally are: 1) the jack influence curves, 2) the linearity range of the jack influence curves as a function of jack deflection, and 3) confirmation of the principle of superposition with respect

to the jack influence curves. Each of these will be discussed in turn.

1. JACK INFLUENCE CURVES

The experimental jack influence curves were obtained by deflecting the i^{th} ($i = 1, 2, \dots, 10$) pair of jacks symmetrically about the tunnel centerline. A deflection of +0.200 inches was used in each case (Fig. 4 denotes sign convention). The experimental jack influence curves were obtained by subtracting the Mach number distribution obtained when all the jacks had zero trim deflection from the centerline Mach number distribution resulting from deflecting the i^{th} pair of jacks +0.200 inches. The resulting data were then divided by two and are presented as Π_{M_x} per 0.1 inch versus centerline station.

The theoretical jack influence curves were obtained using a relaxation technique. The actual nozzle is a plate supported at a number of points by jacks. It is three dimensional and has both transverse and longitudinal deflections under load. However, as a first approximation, the plate was considered as a two dimensional beam with a series of point supports. The problem was then to determine the local slope along the plate if the jack ordinates are known. Once the local slope distribution was known for deflecting the i^{th} jack a unit amount the assumption was made that the local slope was propagated along characteristics lines to the tunnel centerline. By then knowing the $d\theta/dM$ relationship the theoretical Π_{M_x} was obtained.

Figs. 12 and 13 present the experimental and theoretical results at a $M_{CAM} = 1.600$ for jacks 6 and 8 respectively. Figs. 14 and 15 present the experimental and theoretical results at a $M_{CAM} = 1.700$ for jacks 5 and 7. Negative ΔM_x per 0.10 inch denotes a decrease in the local test section Mach number.

2. LINEARITY RANGE

The range of linearity of the jack influence curves, as a function of jack deflection, was investigated to determine how rapidly non-linear effects might be encountered. To obtain the linearity data the theoretical and experimental jack influence curves were integrated as indicated on Figs. 16 and 17 for jack No. 6 at $M_{CAM} = 1.600$. Fig. 16 presents the integrated values plotted versus jack deflection. Fig. 17 presents the normalized linearity data (experimental integrated value divided by corresponding theoretical integrated value) plotted versus jack deflection. From these data it appears that any deviation from linear results is less than the data reduction accuracy. Reference 1 notes that deviation from linear results is gradual; therefore as the maximum jack deflection used to obtain the experimental short nozzles was approximately 0.6 inches, any non-linear effects can be considered small.

3. SUPERPOSITION DATA

An investigation of how various combinations of jack influence curves superimposed was then undertaken to confirm the initial assumption required in the Influence Method. Two cases are presented: 1) At a $M_{CAM} = 1.700$ Fig. 18 presents a comparison of the theoretical and experimental results for jack 6

deflected ± 0.20 inches, and 2) at a $M_{CAM} \approx 1.700$ Fig. 19 presents a comparison of the theoretical and experimental results for deflecting jack number 6 and jack number 8 ± 0.20 inches simultaneously with data for deflecting jack number 6 and jack number 8 ± 0.20 inches independently and adding the results. These two cases confirm experimentally that various combinations of jack influence curves can be added linearly.

D. SHORT NOZZLE DISTRIBUTIONS

Once the fundamental parameters of the Influence Method had been confirmed experimentally the next step was to pick the region of the nozzle in which the Influence Method was to be applied. The boundaries of this region are the centerline Mach number distribution for the present CWT nozzle and the centerline Mach number distribution for the limiting theoretical flexible plate nozzle of the CWT type, i. e., a Foelsch nozzle where $\theta_{1P}/\theta_i = \theta_i/\omega_i = 1.00$. Arbitrary centerline Mach number distributions which denote various short nozzles between the present CWT nozzle and the limiting Foelsch nozzle were then chosen. Fig. 26 presents the centerline Mach number relationship between the CWT nozzle, the limiting Foelsch nozzle, and the various arbitrary distributions for $M_{CAM} \approx 1.600$ and $M_{CAM} \approx 1.700$. It was determined that this region of the nozzle could be influenced by deflecting jacks 5 - 9 without effecting the sonic throat conditions. Various combinations of these jacks (i. e. 5 - 9, 6 - 9) were used in the Influence Method.

Figs. 20, 21 and 22 present the resulting short nozzle distributions at $M_{CAM} \approx 1.600$. The solid lines denote the present CWT centerline Mach number distributions for $M_{CAM} \approx 1.600$ using standard trim settings. These solid line distributions represent the basis for the short nozzle investigation. The dashed lines indicate the arbitrary short nozzle centerline distributions (A, B---F) which, by using the Influence Method, we desire to obtain. The symbols indicate how short a nozzle was actually obtained for each of the arbitrary distributions and jack combinations used.

Figs. 23, 24 and 25 present the resulting short nozzle distributions for $M_{CAM} \approx 1.700$. The definitions of lines and symbols have similar meanings as discussed for $M_{CAM} \approx 1.600$.

The experimental results indicate that at both $M_{CAM} \approx 1.600$ and $M_{CAM} \approx 1.700$ the CWT flexible plate nozzle can be shortened. These results correspond to an increase of approximately 35% in usable testing length (Fig. 2). However, as the nozzle is shortened the undesirable Mach number variation, in the region occupied by models, increases from ± 0.005 to approximately ± 0.015 (Figs. 22 and 25).

Figs. 20-22 for $M_{CAM} \approx 1.600$ and Figs. 23-25 for $M_{CAM} \approx 1.700$ indicate that no substantial progress was made in shortening the nozzle until the E and F distributions were attempted. This appears to be independent of whether four or five jack combinations were used in the Influence Method. The explanation of this appears to be associated with the position of the

inflection point with respect to the jack location but insufficient data prevent the verification of this hypothesis.

V. CONCLUSIONS

The Influence Method was successfully applied to shortening the CWT flexible plate nozzle. The usable testing length at both $M_{CAM} \approx 1.600$ and $M_{CAM} \approx 1.700$ was increased by approximately 35%. However as the nozzle approached the limiting Foelsch nozzle the undesirable Mach number variation, in the region occupied by models, increased from +0.005 to +0.015.

It was determined that the experimental short nozzle distributions agreed very well with the predicted results obtained from the Electrodata Datatron. These results, which have not been presented, indicate that the non-linear effects encountered in the use of the Influence Method are small. This enabled the investigation, in part, to be made without the need of actual experimental confirmation.

The initial assumptions made in the Influence Method (i. e. that the jack influence curves are linear with respect to the jack deflection and that the jack influence curves satisfy the principle of superposition) were confirmed experimentally for the range of jack deflections used.

The results indicate that further investigation should be made in order to evaluate more completely the usefulness of applying this technique to shortening supersonic flexible plate nozzles. First, shorter nozzles should be attempted to ascertain how short the nozzle can be made before the aerodynamic limit, in the form of compression waves, is reached. Secondly,

the undesirable Mach number variation which appears as a result of shortening the flexible plate nozzle is of the same order of magnitude for either jacks 5-9 or jacks 6-9 used in the Influence Method. This indicates that in order to minimize the undesirable Mach number variation, more jacks would have to be used in the Influence Method. This requires that the jacks farther upstream (i. e. jacks 3 and 4) would have to be used. However, the use of jacks 3 and 4 influence the sonic throat conditions in two ways. First, by changing the area ratio the entire flow field of the nozzle is affected, and second, the use of the upstream jacks raises the plate stress level at the throat and the maximum allowable plate stress may be exceeded. Therefore, a more complete study using the upstream jacks should be attempted if further improvement is desired.

REFERENCES

1. MacDermott, Wm., The Correction of Flexible Plate Supersonic Nozzle Contours by Influence Methods. AEDC-TN-53-8. (Dec. 1953.)
2. Puckett, Allen, Design and Operation of a 12" Supersonic Wind Tunnel, IAS Preprint #160. (July 1948.)
3. Huebner, Danny, CWT Nozzle Correction Theory as Applied to Flexible Plate Nozzles. CWT Rep. T-69. (Unpublished)
4. Riise, Harold N., Flexible-Plate Nozzle Design for Two-Dimensional Wind Tunnels. J.P.L. Rep. 20-74. (June 1954.)
5. Millikan, Clark B., AE201, Compressible Fluid Notes as of September 1956.

APPENDIX I NOTATION

A. NOTATION USED FOR THE INFLUENCE METHOD

- a, b Integration limits measured on tunnel centerline
- x Axial distance in feet measured along tunnel centerline
- $\mathcal{E}_M(x)$ Difference between the desired centerline Mach number distribution and the C_L distribution as measured experimentally in the region $a - b$
- $\mathcal{E}_\theta(x)$ Measured centerline flow direction variation between a and b
- $\Delta_{i,j}$ Jack deflection in inches
- $()_i$ Ceiling jack station ($i = 1, 2 \dots n$)
- $()_j$ Floor jack station ($i = 1, 2 \dots m$)
- $[\delta\theta_w(x)]_{i,j}$ Change in plate slope due to unit $\Delta_{i,j}$
- $I_{M_{i,j}}$ Change in Mach number on tunnel C_L due to unit $\Delta_{i,j}$
- $\Pi_{M_i} = I_{M_i} + I_{M_j}$ when $i = j$
- $I_{\theta_{i,j}}$ Change in flow direction on tunnel C_L due to unit $\Delta_{i,j}$
- $\Pi_{\theta_i} = I_{\theta_i} + I_{\theta_j}$ when $i = j$

B. NOTATION USED FOR THE THEORETICAL
LENGTH ESTIMATES

- θ Flow inclination
- ν Prandtl Meyer angle
- X Axial distance in feet
- Y Vertical distance in feet
- γ Area ratio = A/A^*
- $H/2$ Test section height in feet
- μ Mach angle

Subscripts:

- i Inflection point
- t Throat
- e Exit
- w Points on wall downstream of inflection point
- wP Wall point at which characteristic passing through θ_{IP} intersects
- i Points along arc of source flow
- IP Point on arc of source flow where last partially cancelled wave intersects

C. NOTATION USED TO DESCRIBE
CONFIGURATIONS TESTED

- M_{CAM} Mach number as recorded from the cam dial in the CWT control room
- STD. Denotes *standard trim settings (symmetric)*
- A,B...F Denotes trim settings used to obtain a particular arbitrary distribution
- () Denotes an iteration solution

Subscripts:

- ()_u Denotes base distribution was obtained using zero trim settings
- ()_c Denotes base distribution was obtained using standard trim settings
- ()_{()₆} $M_{CAM} = 1.600$
- ()_{()₇} $M_{CAM} = 1.700$

Superscripts:

- () Denotes jacks 6-9 used in influence technique
- ()['] Denotes jacks 5-8 used in influence technique
- ()^{''} Denotes jacks 5-9 used in influence technique

APPENDIX II RUN SCHEDULE

(CWT REP. K-292)

Run	Pt.	M _{CAM}	Trim Config.	T _o °F	P _o cm. Hg.	Date
1	1		Zero Point	100	24.46	8-21-57
	2	1.700	Zero	146	28.55	8-21-57
	3	1.700	No Good	147	28.58	8-21-57
	4	1.700	No Good	145	28.67	8-21-57
	5	1.700	No Good	146	28.82	8-21-57
	6	1.700	Ac ₇	147	29.03	8-21-57
	7	1.700	No Good	147	29.12	8-21-57
	8	1.700	Au ₇	146	29.12	8-21-57
	9	1.700	Bu ₇	146	29.27	8-21-57
	10	1.700	Cu ₇	146	29.37	8-21-57
	11	1.700	Bc ₇	146	29.51	8-21-57
	12	1.700	Cc ₇	147	29.58	8-21-57
	13	1.700	Zero	145	29.61	8-21-57
	14	1.700	Au ^s ₇	145	29.67	8-21-57
	15	1.700	Bu ^s ₇	146	29.72	8-21-57
	16	1.700	Cu ^s ₇	146	29.79	8-21-57
	17	1.700	Ac ^t ₇	146	29.91	8-21-57
	18	1.700	Bc ^t ₇	146	29.99	8-21-57
	19	1.700	Cc ^t ₇	146	30.01	8-21-57
	20	1.700	Zero	146	30.05	8-21-57
	21			Zero Point	98	23.62
2	1		Zero Point	88	23.29	8-21-57
	2	1.600	Zero	141	30.13	8-21-57
	3	1.600	Au ₆	141	30.30	8-21-57

Run	Pt.	M _{CAM}	Trim Config.	T _o °F	P _o cm. Hg.	Date
2	4	1.600	Bu ₆	141	30.43	8-21-57
	5	1.600	Cu ₆	141	30.55	8-21-57
	6	1.600	Ac ₆	141	30.68	8-21-57
	7	1.600	Bc ₆	141	30.75	8-21-57
	8	1.600	Cc ₆	141	30.83	8-21-57
	9	1.600	Zero	141	30.85	8-21-57
	10	1.600	No Good	141	30.96	8-21-57
	11	1.600	Au' ₆	141	30.98	8-21-57
	12	1.600	Bu' ₆	141	31.00	8-21-57
	13	1.600	Cu' ₆	141	31.11	8-21-57
	14	1.600	Ac' ₆	141	31.15	8-21-57
	15	1.600	Bc' ₆	141	31.20	8-21-57
	16	1.600	Cc' ₆	145	31.23	8-21-57
	17	1.600	Zero	145	31.37	8-21-57
3	1	1.66	STD	145	31.55	8-21-57
	2		Zero Point	103	24.95	8-21-57
4	1		Zero Point	105	21.48	11-27-57
	2	1.700	STD	148	28.39	11-27-57
	3	1.700	Ac ₇ +STD	145	28.44	11-27-57
	4	1.700	Bc ₇ +STD	147	28.58	11-27-57
	5	1.700	Cc ₇ +STD	149	28.72	11-27-57
	6	1.700	Dc ₇ +STD	151	28.84	11-27-57
	7	1.700	Ec ₇ +STD	149	28.23	11-27-57

Run	Pt.	M _{CAM}	Trim Config.	T _o °F	P _o cm. Hg.	Date
4	8	1.700	Fc ₇ +STD	150	29.06	11-27-57
	9	1.700	STD	148	29.08	11-27-57
	10	1.700	Dc'' ₇ +STD	150	29.23	11-27-57
	11	1.700	Ec'' ₇ +STD	149	29.38	11-27-57
	12	1.700	Fc'' ₇ +STD	150	29.51	11-27-57
	13	1.700	STD	150	29.62	11-27-57
	5	1	1.600	STD	145	29.48
2		1.600	Ac ₆ +STD	147	29.61	11-27-57
3		1.600	Bc ₆ +STD	148	29.76	11-27-57
4		1.600	Cc ₆ +STD	145	29.80	11-27-57
5		1.600	Dc ₆ +STD	144	29.90	11-27-57
6		1.600	Ec ₆ +STD	145	29.99	11-27-57
7		1.600	Fc ₆ +STD	145	30.12	11-27-57
8		1.600	STD	146	30.23	11-27-57
9		1.600	Dc'' ₆ +STD	145	30.39	11-27-57
10		1.600	Ec'' ₆ +STD	146	30.49	11-27-57
11		1.600	Fc'' ₆ +STD	146	30.63	11-27-57
12		1.600	STD	146	30.70	11-27-57
13		1.600	IC _{c₆} +STD	146	30.84	11-27-57
14		1.600	IC _{c₆} +STD	146	31.00	11-27-57
15		1.600	IC'' _{c₆} +STD	145	31.16	11-27-57
16			Zero Point		111	24.83

APPENDIX III LIST OF FIGURES

FIGURE	TITLE	PAGE
1	The CWT Supersonic Flexible Plate Nozzle	30
2	Usable Testing Length vs. Mach Number	31
3	Region of Application of the Influence Method	32
4	Sign Convention	32
5	Nozzle Notation Schematic	33
6	Nozzle Length Estimate Notation	33
7	Nozzle Length Estimates, $M_{CAM} = 1.600$	34
8	Nozzle Length Estimates, $M_{CAM} = 1.700$	35
9	Estimated Change in Length of Shortened Nozzle, Case I	36
10	Estimated Change in Length of Shortened Nozzle, Case II	37
11	Estimated Change in Length of Shortened Nozzle, Case III	38
12	Mach Influence Curve for Jack 6 at $M_{CAM} = 1.600$	39
13	Mach Influence Curve for Jack 8 at $M_{CAM} = 1.600$	40
14	Mach Influence Curve for Jack 5 at $M_{CAM} = 1.700$	41
15	Mach Influence Curve for Jack 7 at $M_{CAM} = 1.700$	42
16	Linearity Data as a Function of Δ_i	43
17	Normalized Linearity Data	44
18	Superposition Data, Jack 6 at $M_{CAM} = 1.700$	45
19	Superposition Data, Jacks 6, 8 at $M_{CAM} = 1.700$	46
20	Short Nozzle Distributions Ac_6 , Bc_6 and Cc_6 at $M_{CAM} = 1.600$ (Jacks 6-9)	47
21	Short Nozzle Distributions Dc_6 , Ec_6 and Fc_6 at $M_{CAM} = 1.600$ (Jacks 6-9)	48

22	Short Nozzle Distributions $Dc_6^{\prime\prime}$, $Ec_6^{\prime\prime}$ and $Fc_6^{\prime\prime}$ at $M_{CAM} = 1.600$ (Jacks 5-9)	49
23	Short Nozzle Distributions Ac_7 , Bc_7 and Cc_7 at $M_{CAM} = 1.700$ (Jacks 6-9)	50
24	Short Nozzle Distributions Dc_7 , Ec_7 and Fc_7 at $M_{CAM} = 1.700$ (Jacks 6-9)	51
25	Short Nozzle Distributions $Dc_7^{\prime\prime}$, $Ec_7^{\prime\prime}$ and $Fc_7^{\prime\prime}$ at $M_{CAM} = 1.700$ (Jacks 5-9)	52
26	Relationship of Arbitrary Distributions and Shortest Theoretical Nozzles for $M_{CAM} = 1.600$ and $M_{CAM} = 1.700$	53

GEOMETRIC HEIGHT AT STA. 22.5' = 8.5'
 " " " " " " = 11.0'

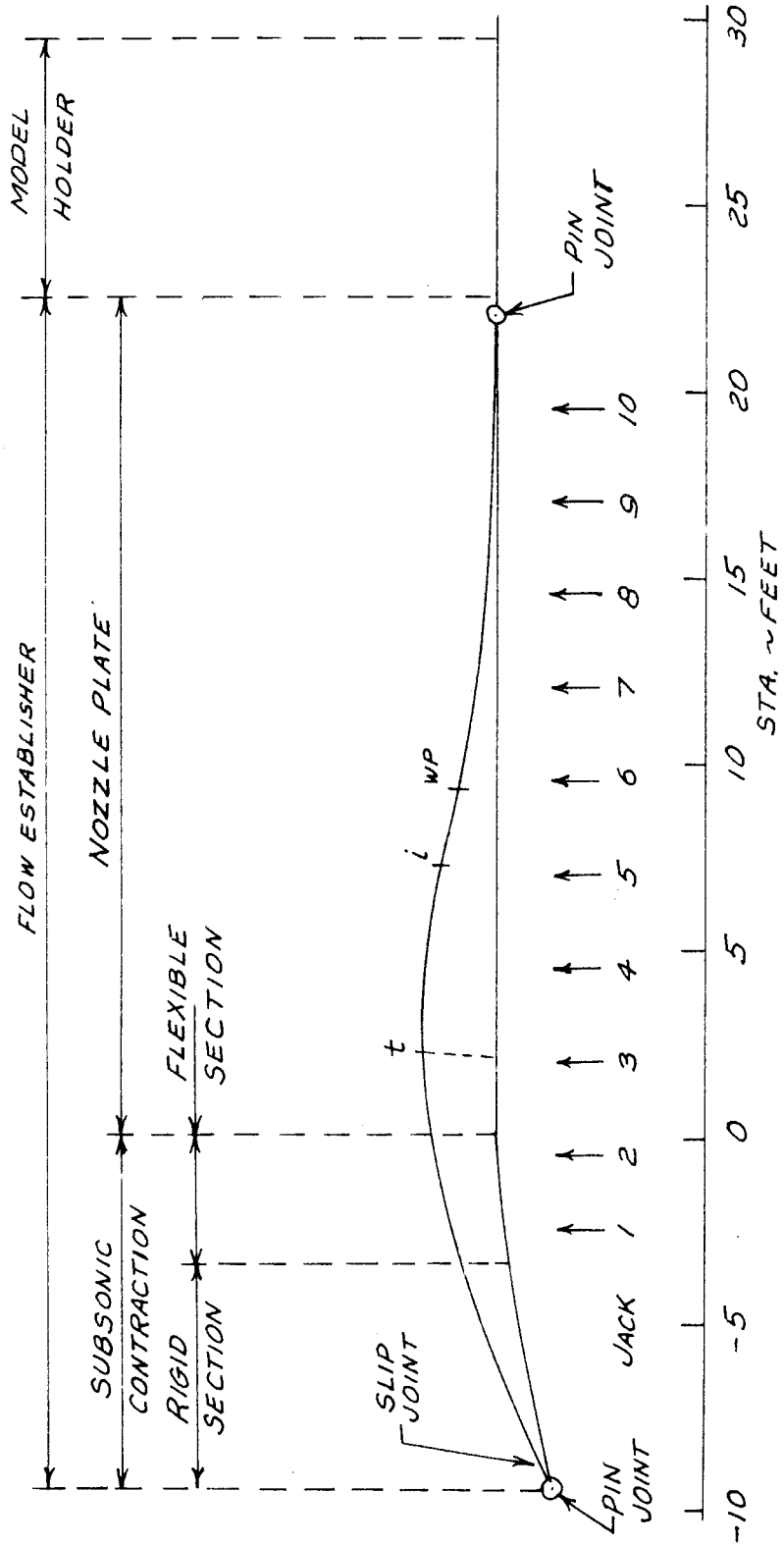


FIGURE 1. THE CWT SUPERSONIC FLEXIBLE PLATE NOZZLE

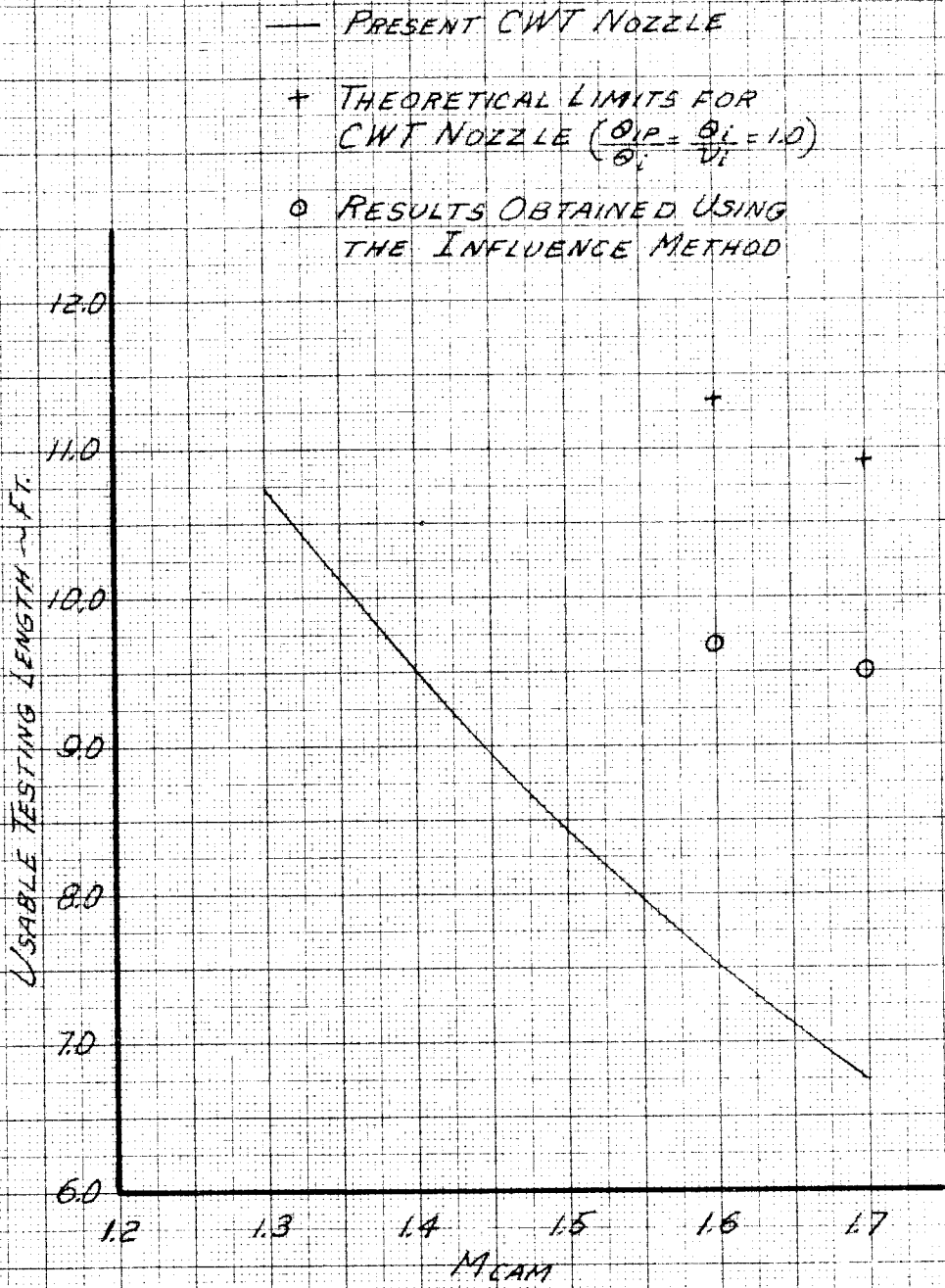


FIGURE 2. USABLE TESTING LENGTH VS. MACH NUMBER

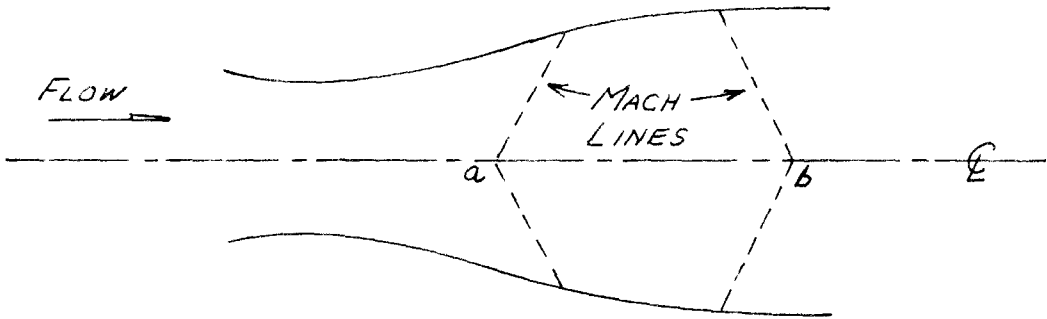


FIGURE 3. REGION OF APPLICATION OF THE INFLUENCE METHOD

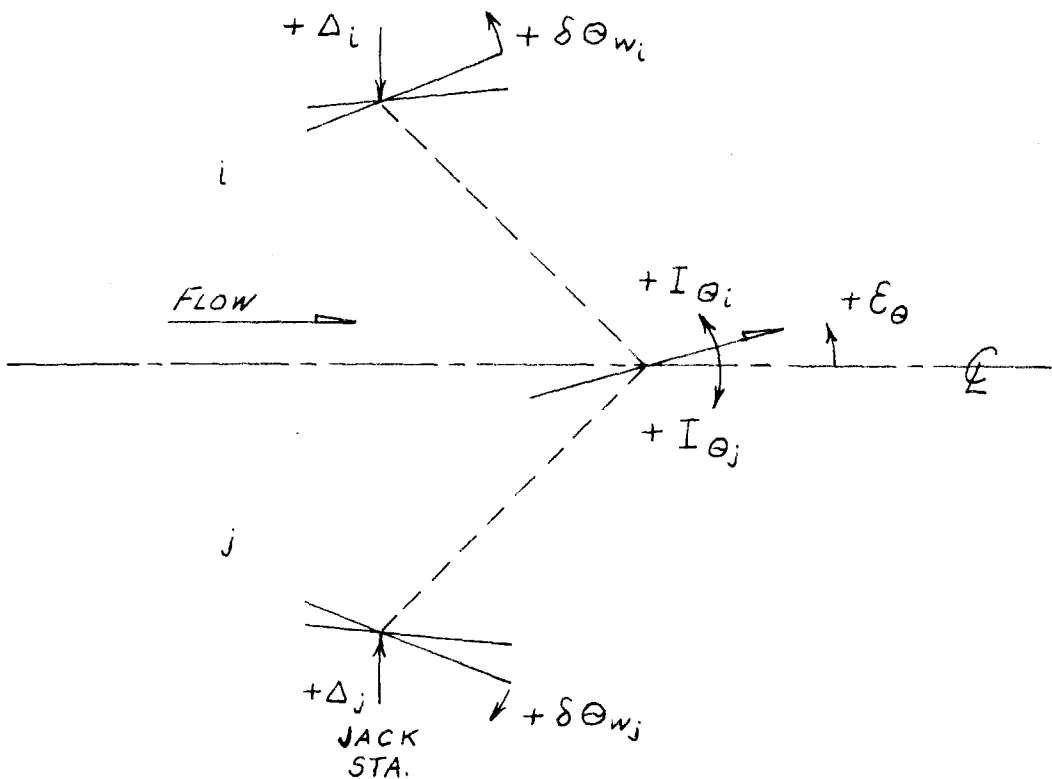


FIGURE 4. SIGN CONVENTION

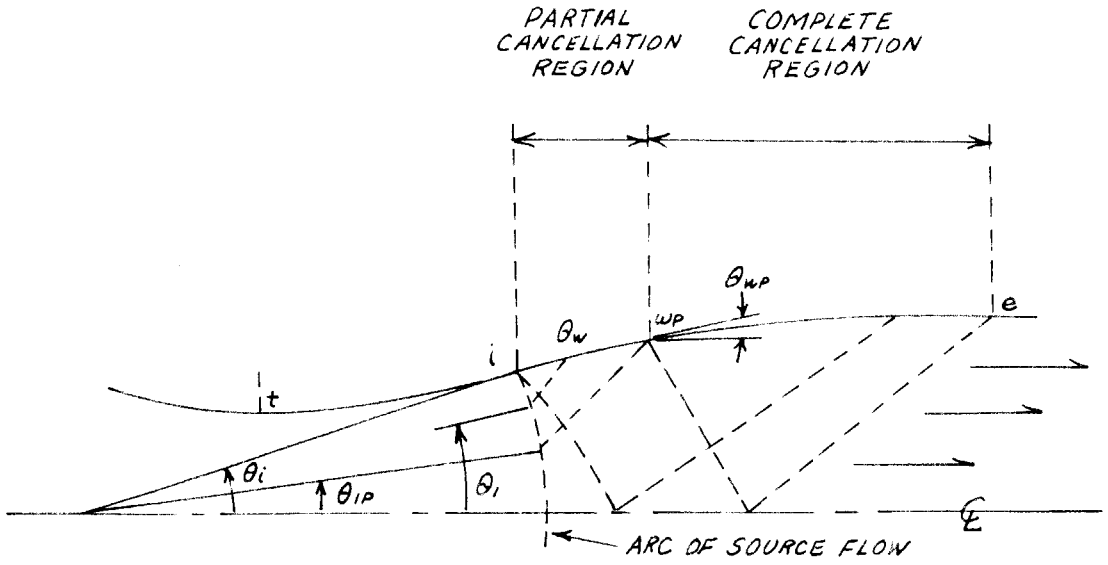


FIGURE 5. NOZZLE NOTATION SCHEMATIC

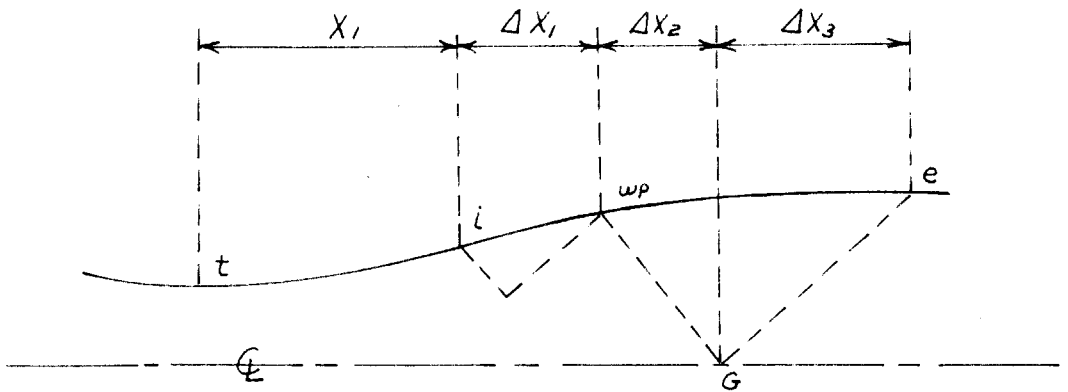


FIGURE 6. NOZZLE LENGTH ESTIMATE NOTATION

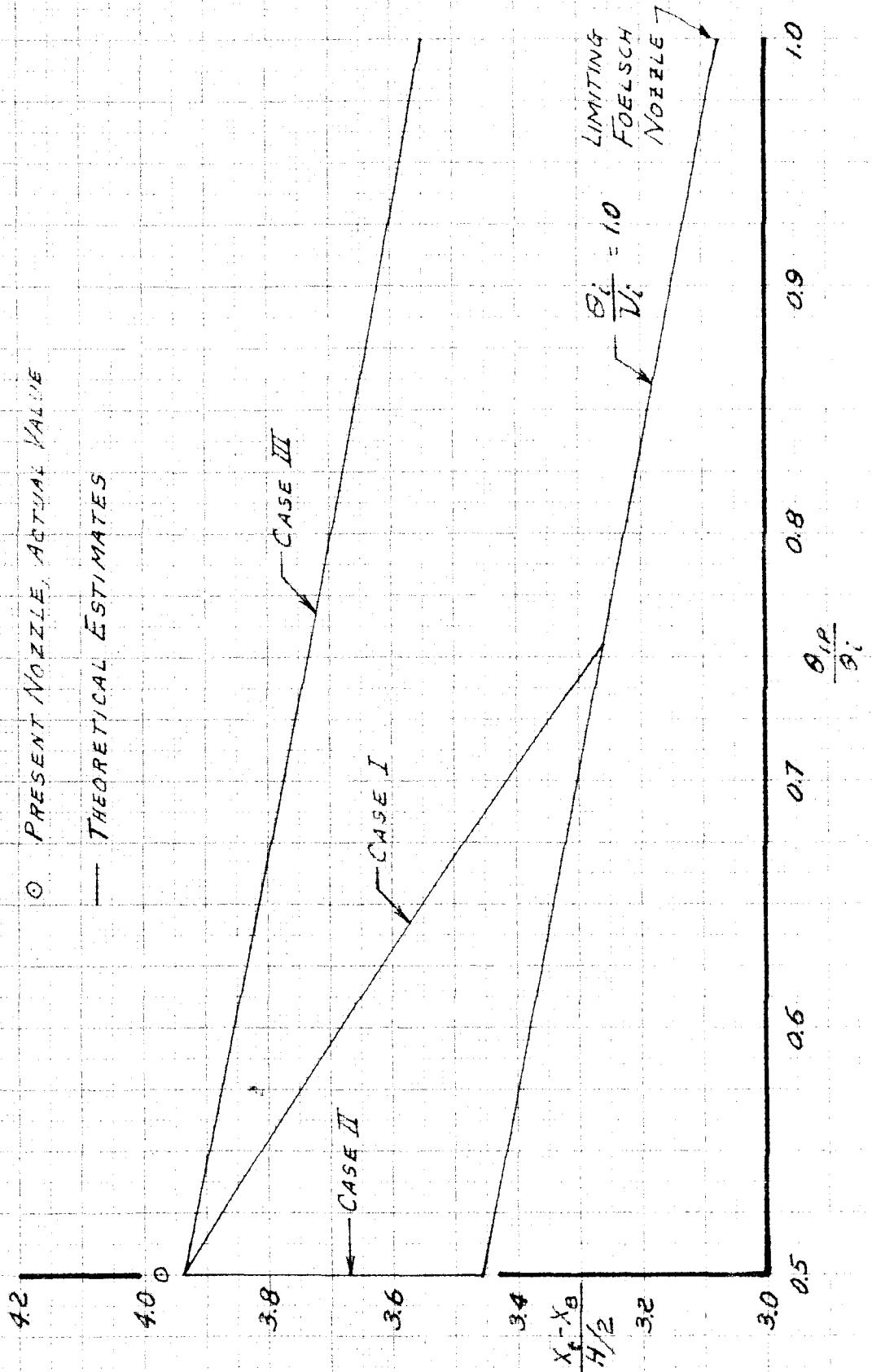


FIGURE 7. NOZZLE LENGTH ESTIMATES, $M_{CAM} = 1.600$

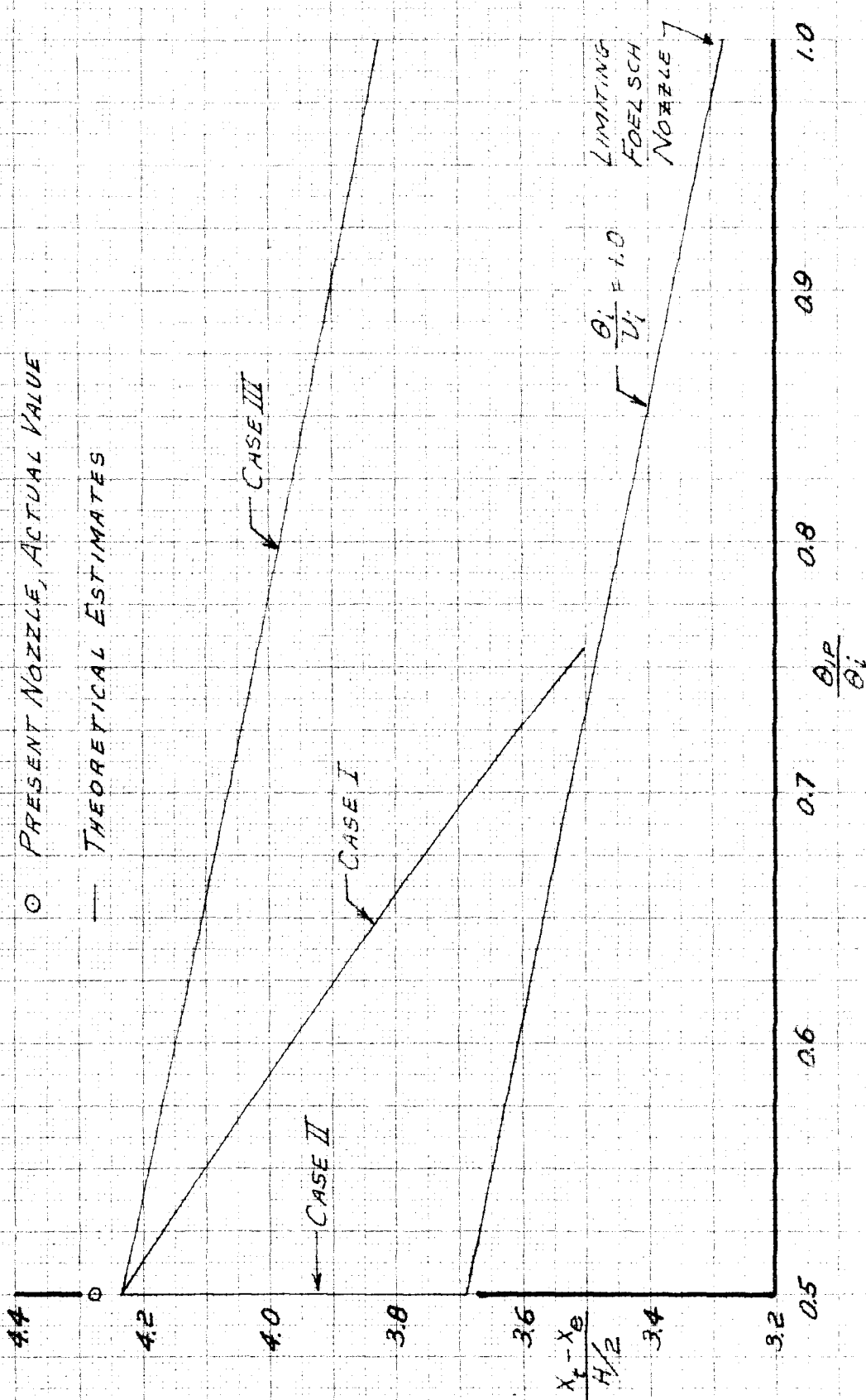


FIGURE 8. NOZZLE LENGTH ESTIMATES, $M_{CAM} = 1.700$

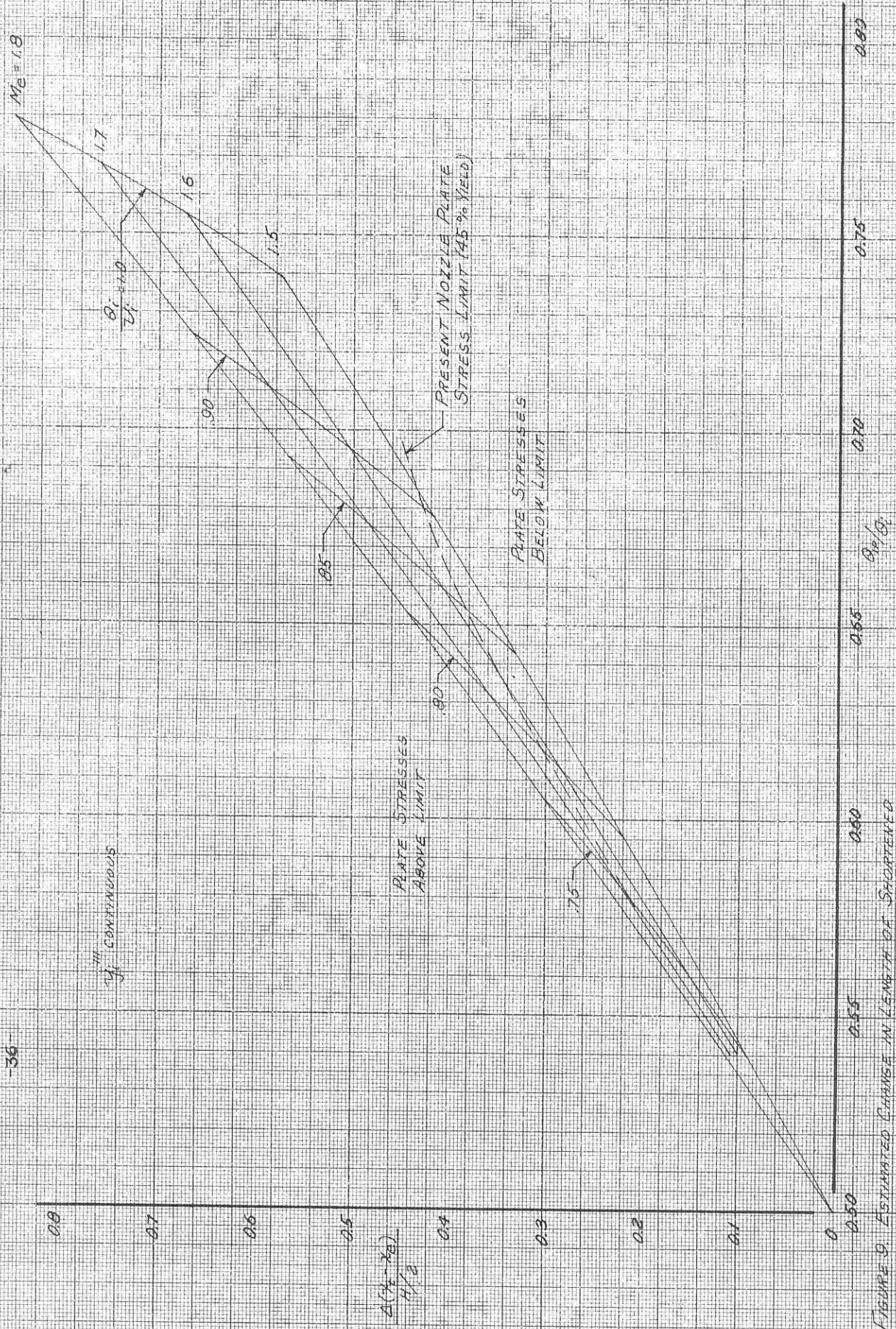


FIGURE 9. ESTIMATED CHANGE IN LENGTH OF SHORTENED NOZZLE, CASE I

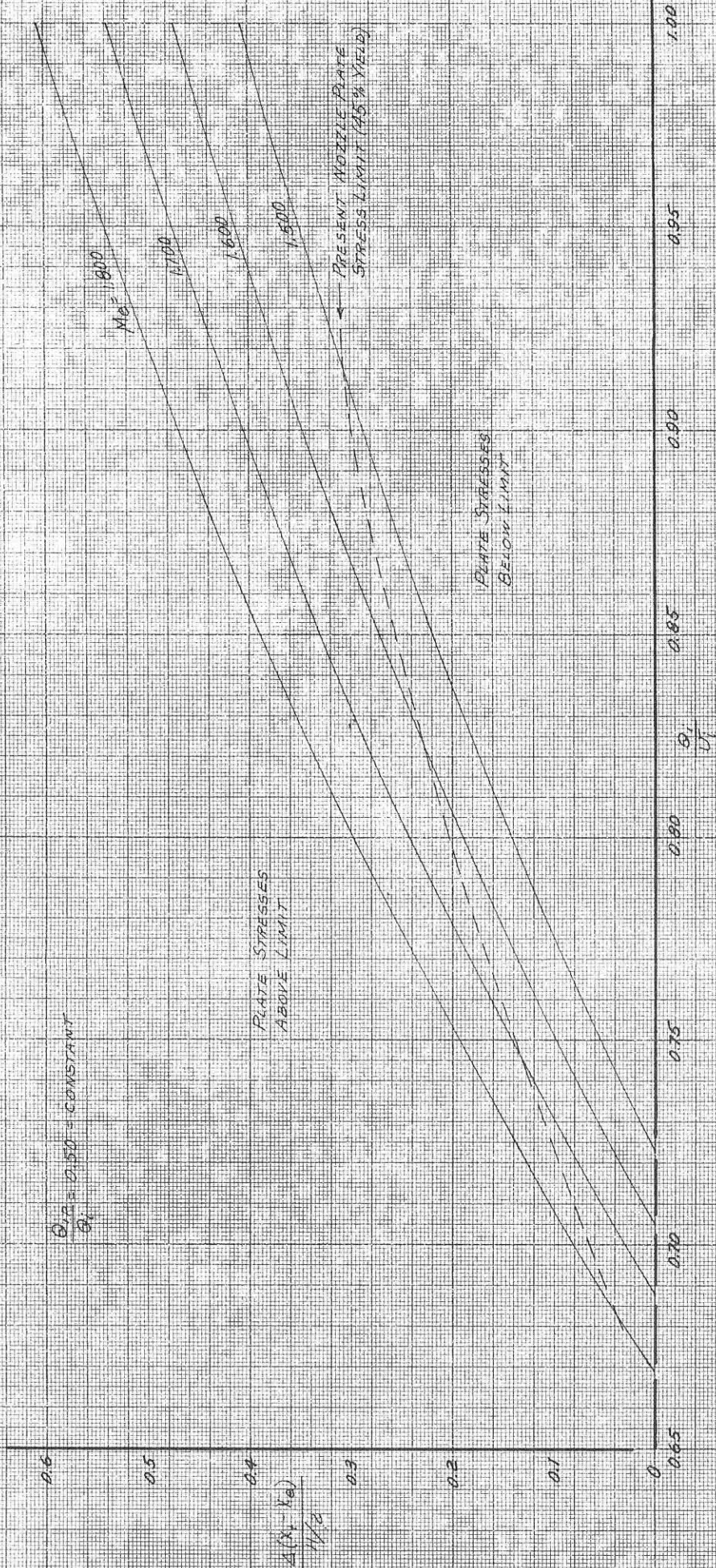


FIGURE 10. ESTIMATED CHANGE IN LENGTH OF SHORTENED NOZZLE, CASE II

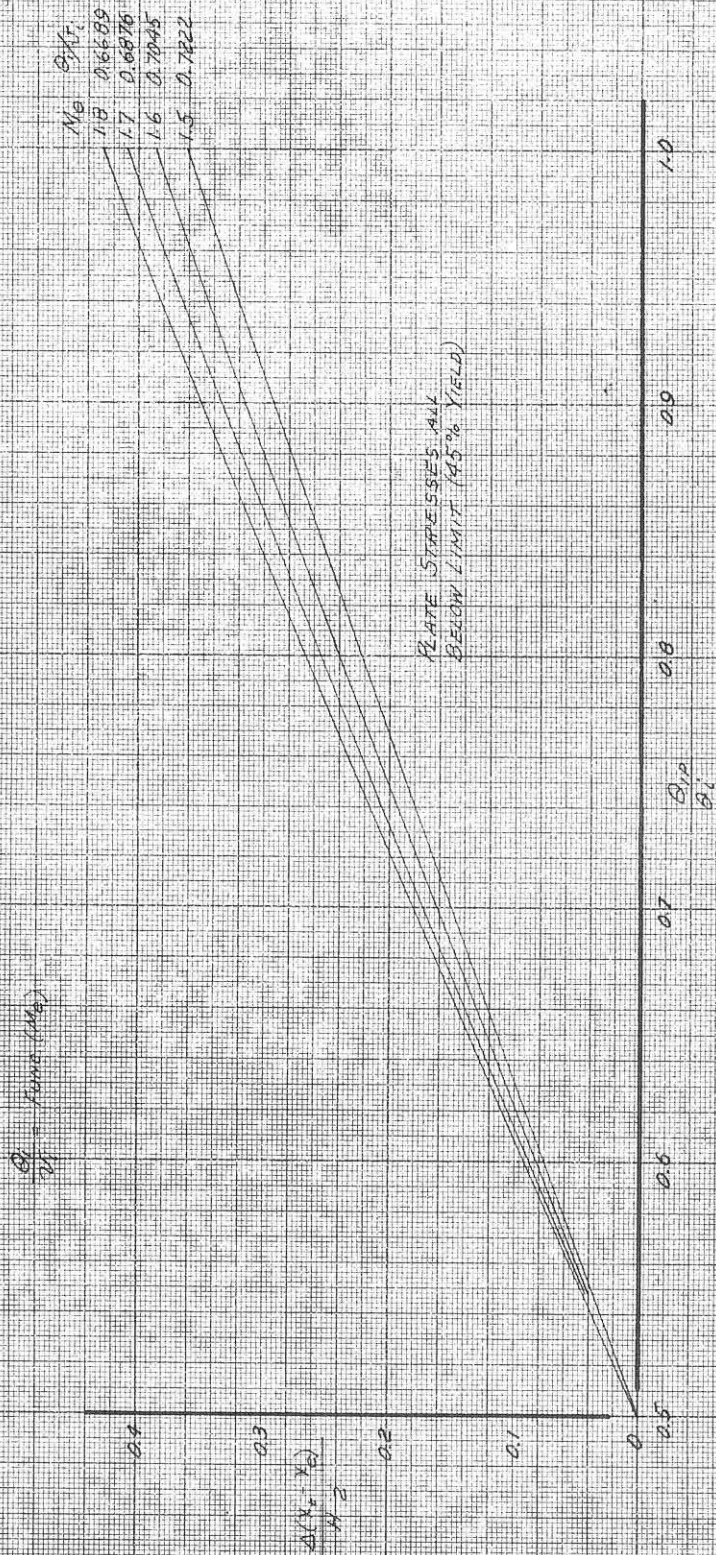


FIGURE 11. ESTIMATED CHANGE IN LENGTH OF SHORTENED NOZZLE, CASE III

FIGURE 12. MACH INFLUENCE CURVES FOR VACT 6
AT $M_{CAN} = 4.600$

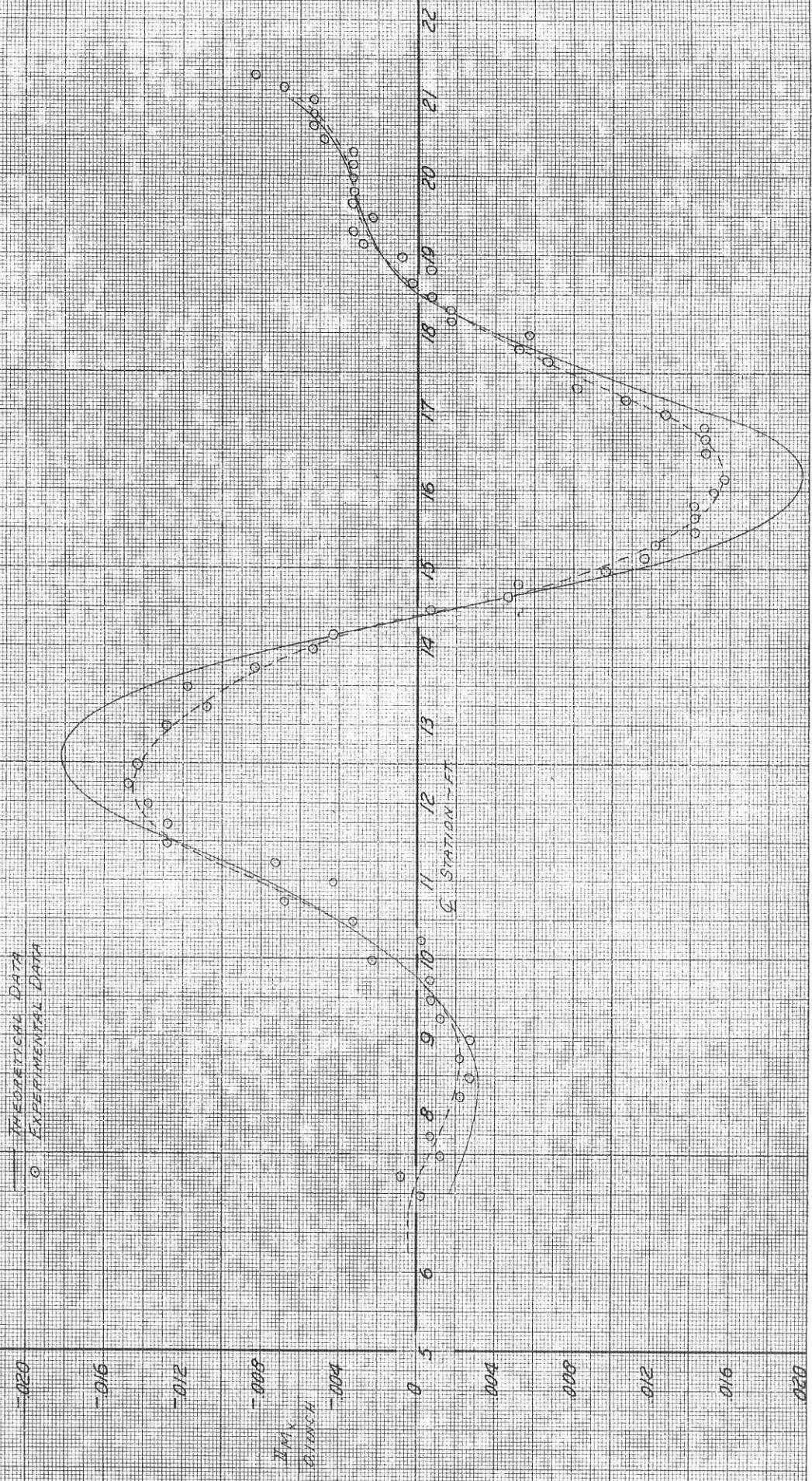


FIGURE 13. MACH NUMBER CURVES FOR JACA 8
AT $M_{\infty} = 4.500$



FIGURE 1A MACH INFLUENCE CURVES FOR JACK 5
AT $M_{CAM} = 1.100$

— THEORETICAL DATA
○ EXPERIMENTAL DATA

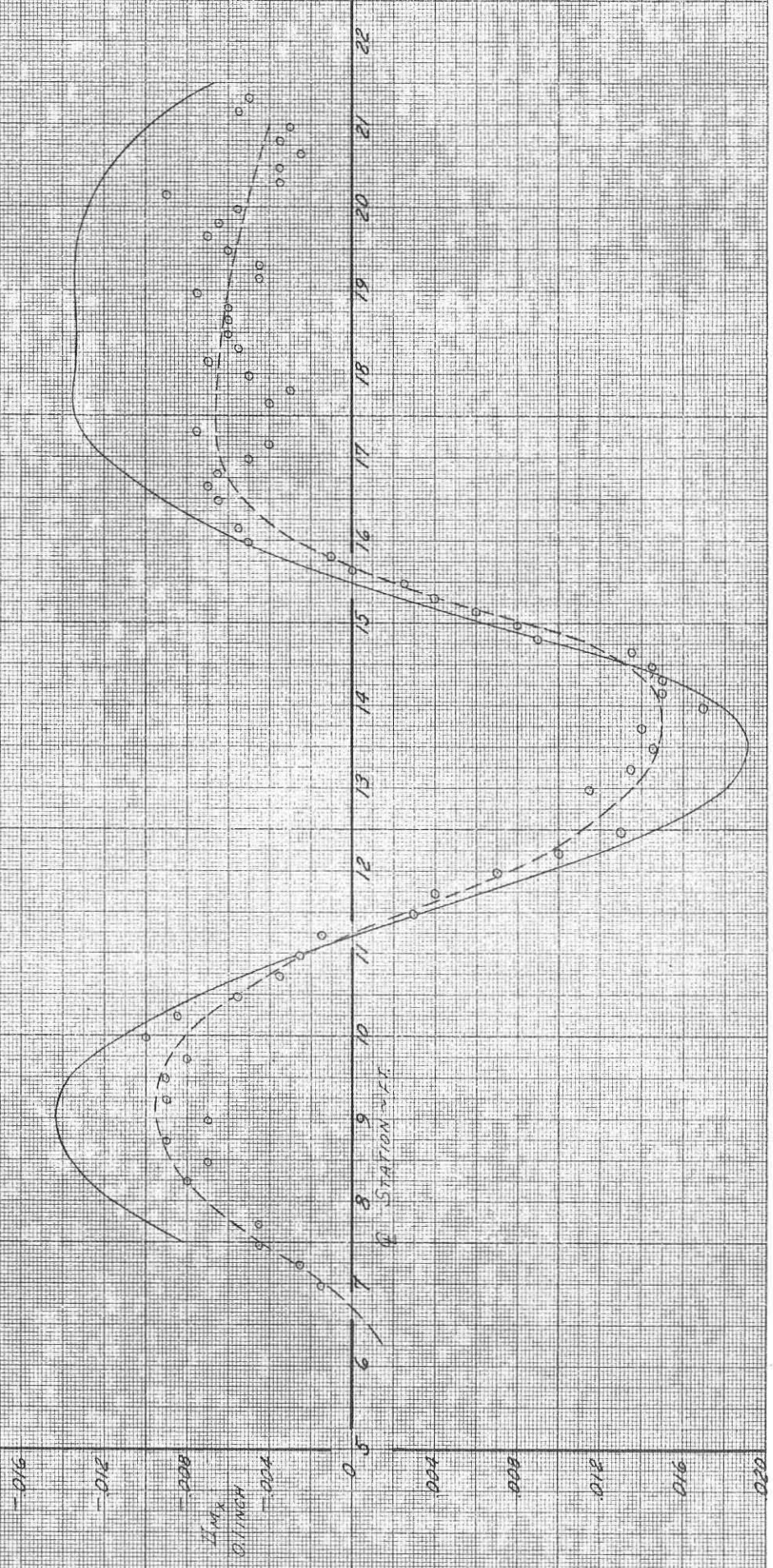
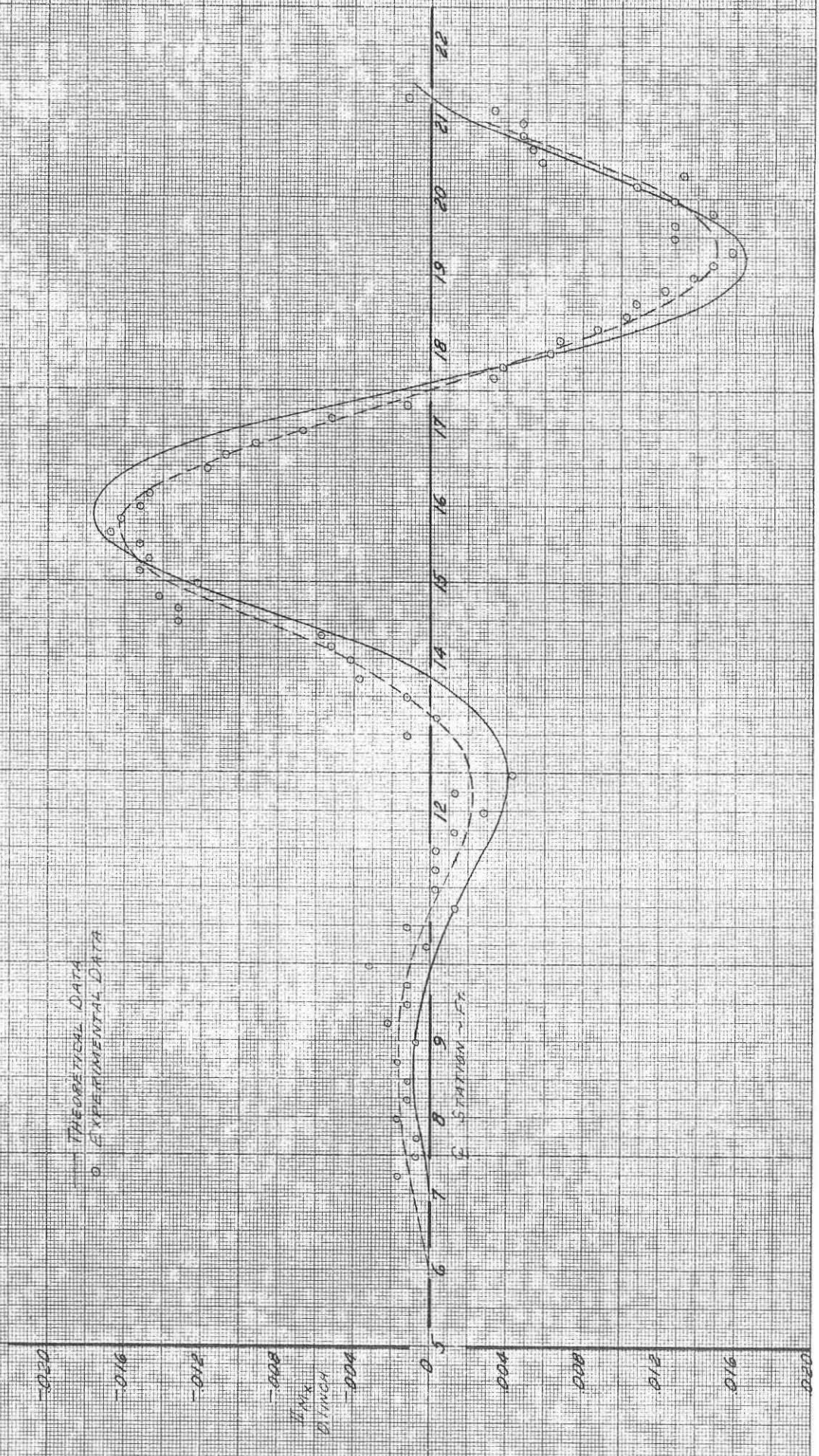


FIGURE 15. INCH INFLUENCE CURVES FOR JACK 1
AT MEAN = 1.700



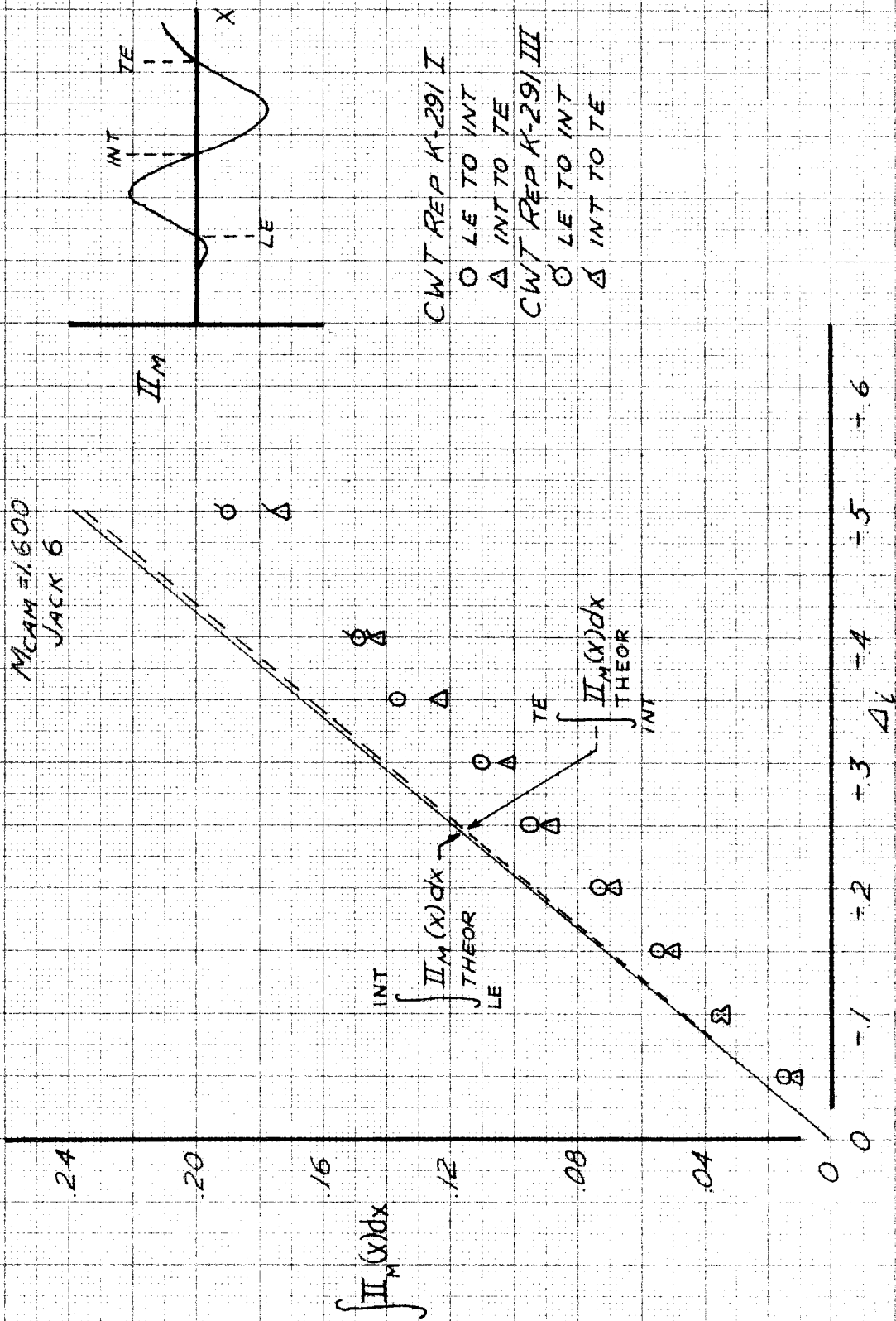
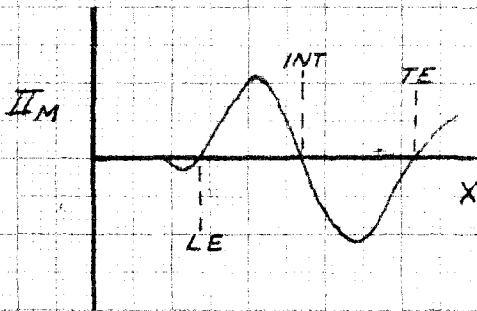


FIGURE 16. LINEARITY DATA AS A FUNCTION OF Δi



INT

$$\int_{LE}^{INT} II_M(x) dx = 0.04771$$

THEOR

TE

$$\int_{TE}^{INT} II_M(x) dx = 0.04714$$

THEOR

MICROM = 1.600
JACK No. 6

CWT REP K-291 I

○ LE TO INT

△ INT TO TE

CWT REP K-291 III

○ LE TO INT

△ INT TO TE

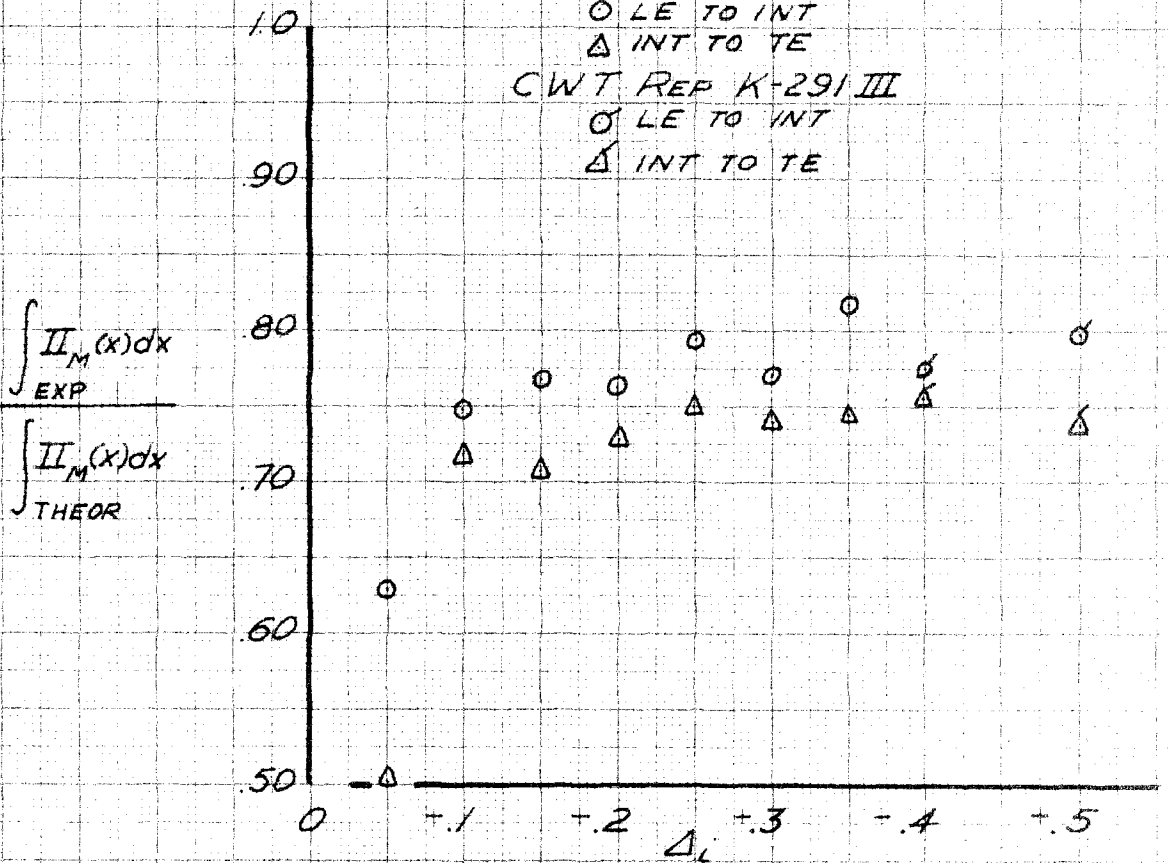


FIGURE 17. NORMALIZED LINEARITY DATA

FIGURE 18. SUPERPOSITION DATA, JACK 6 AT M_{CAW} = 1.700

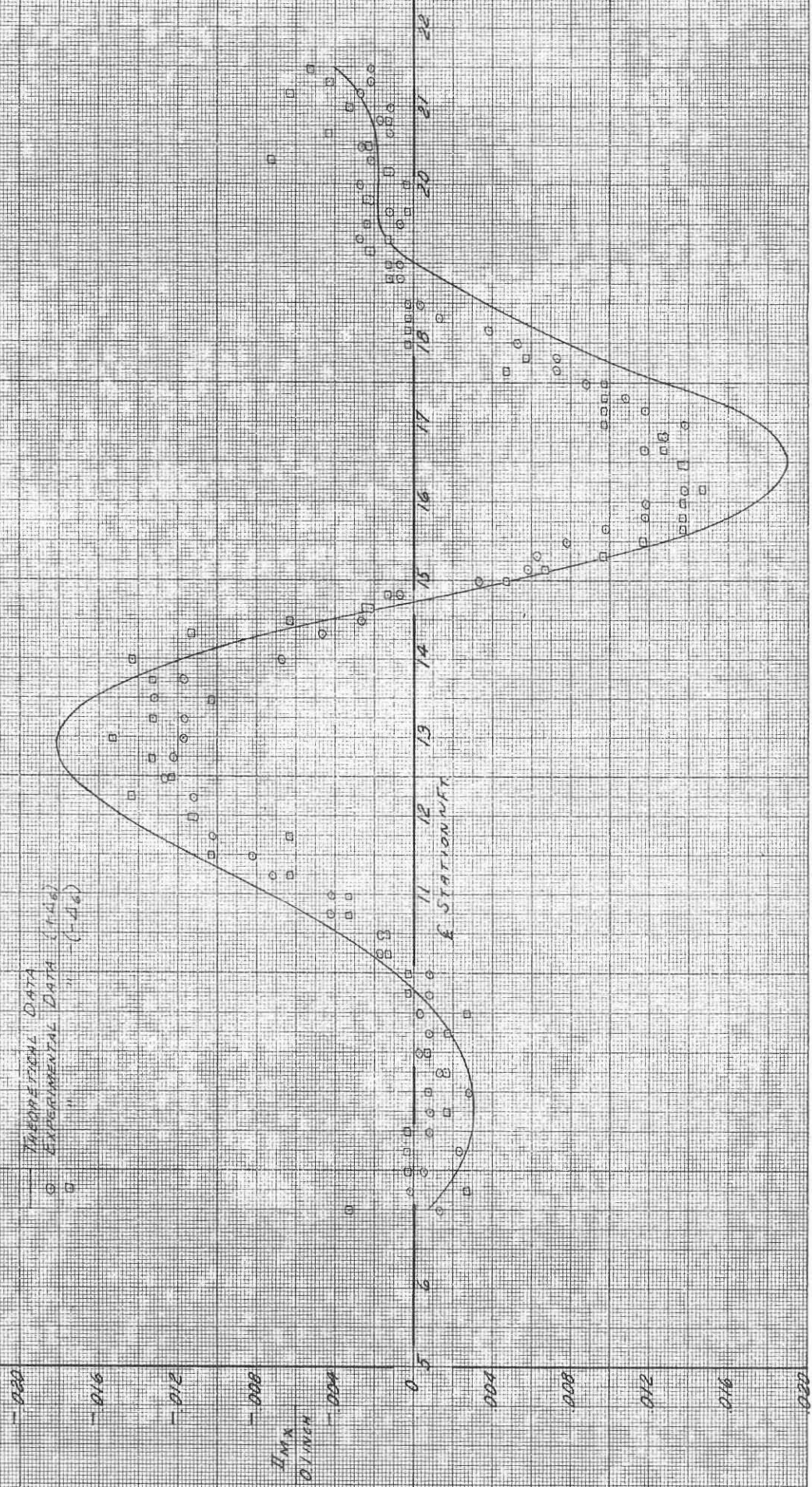


FIGURE 10 SUPERPOSITION DATA, VACUUM BAND BAY $M_{\text{eff}} = 1.700$

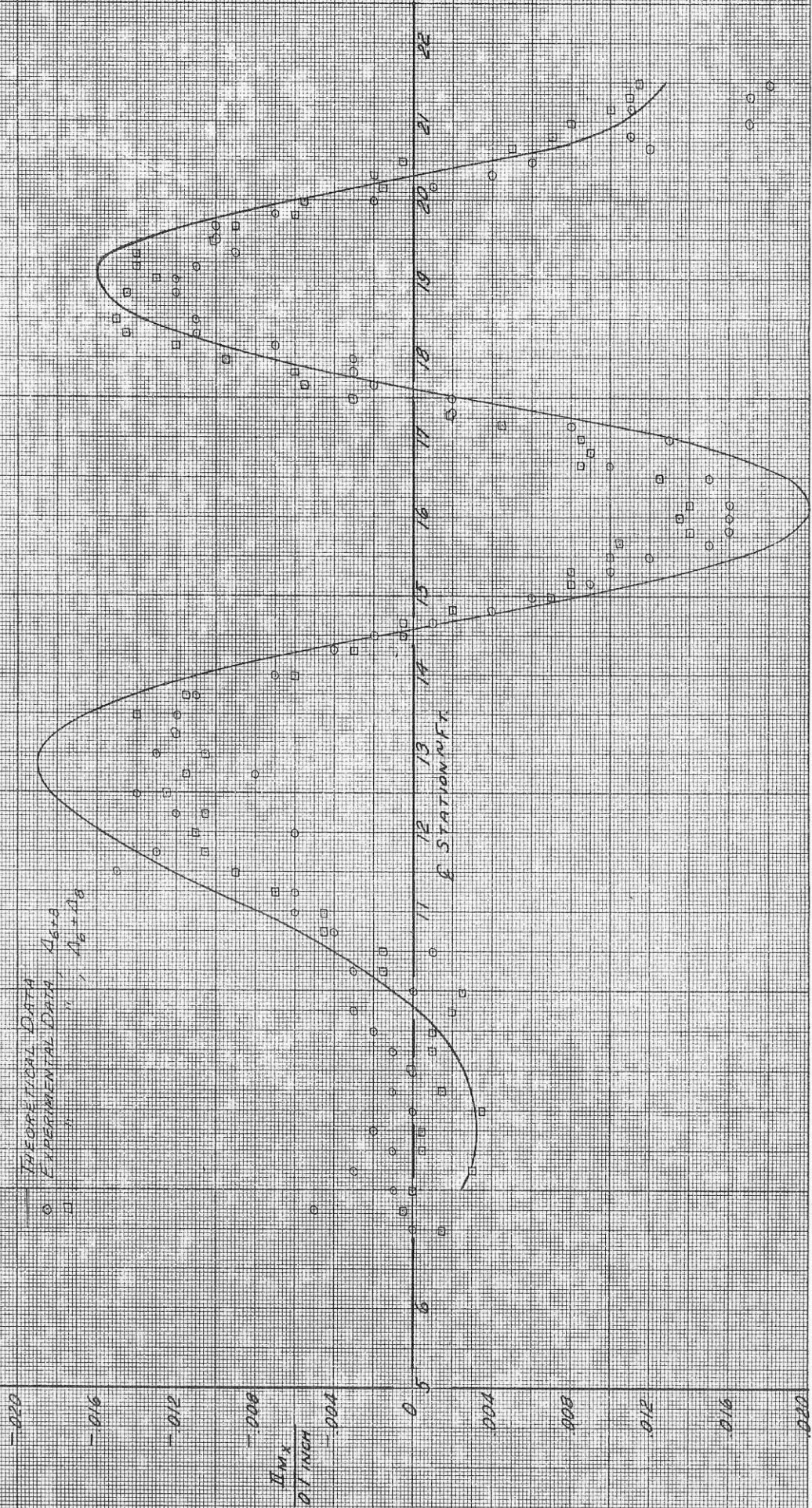


FIGURE 20. SHROFF NOZZLE DISTRIBUTIONS A_6 , B_6 , AND C_6 AT $M_{CAM} = 1600$ (PACKS 6-9)

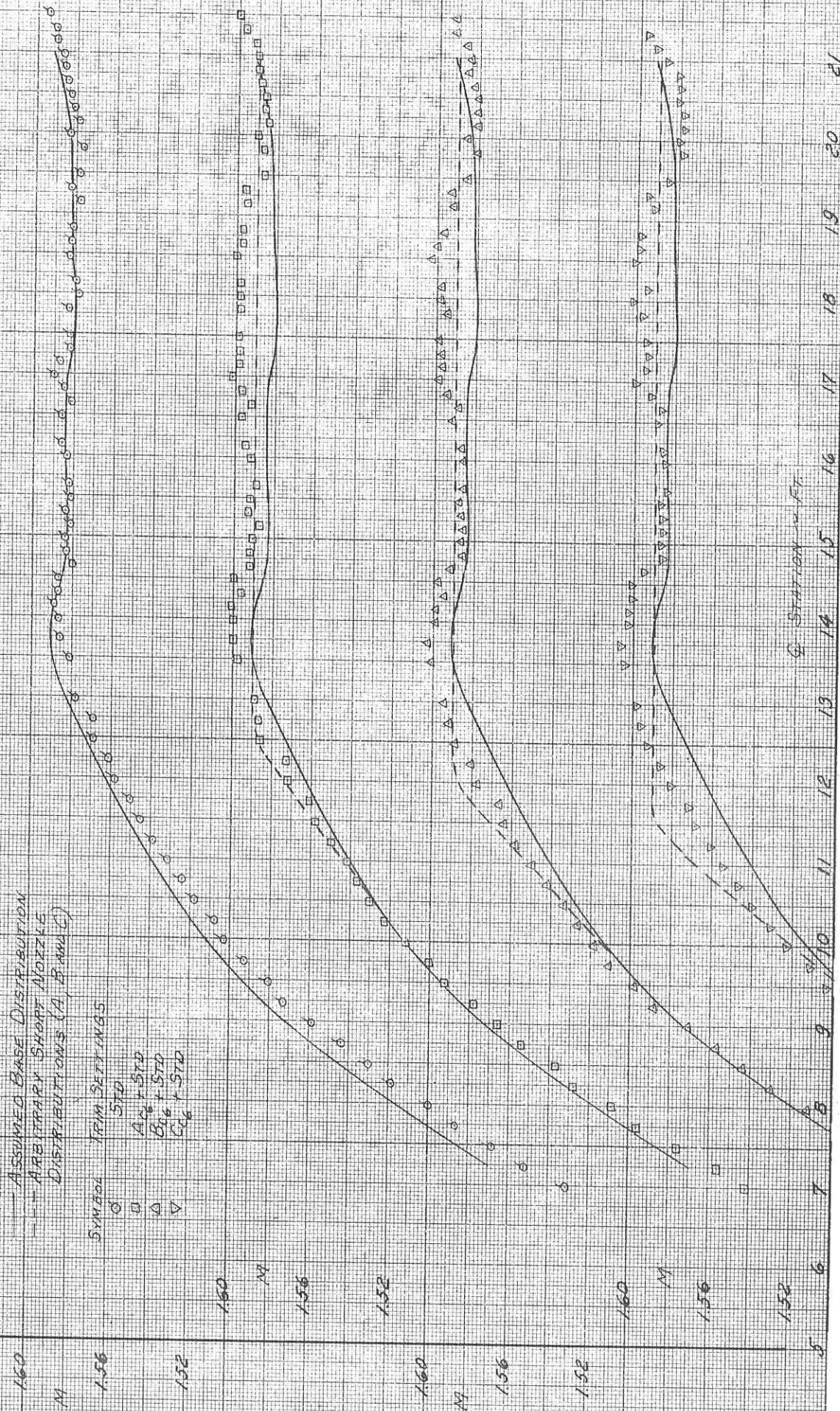


FIGURE 21. SHORT NOZZLE DISTRIBUTIONS D_{16} , E_{16} AND F_{16} AT $M_{CAN} = 1.600$ (WHEAS 6-9)

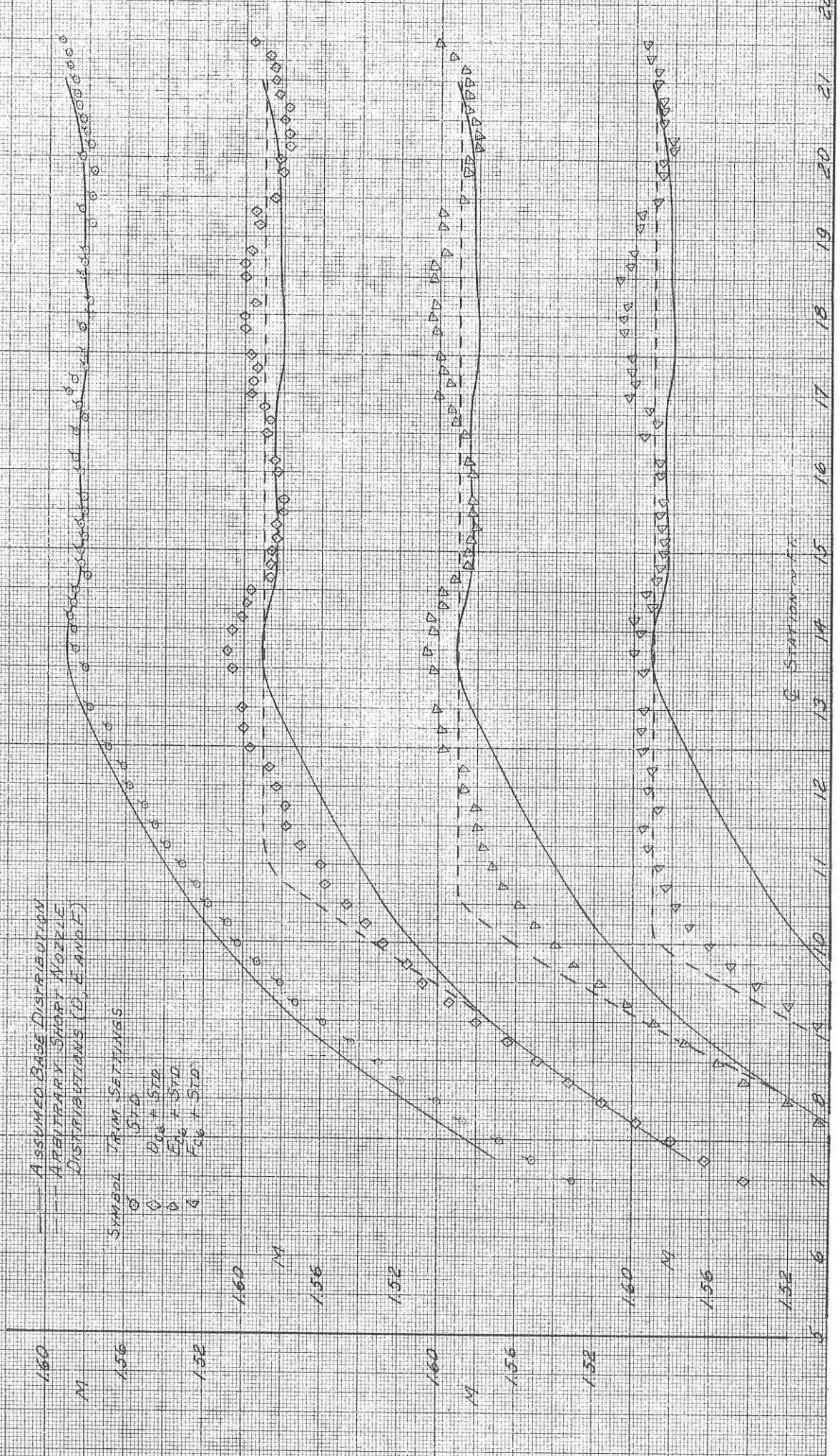


FIGURE 22. SHORT NOZZLE DISTRIBUTIONS Q_{16}^1 , F_{16}^1 AND F_{16}^4 AT MEAN = 1600 (JACKS 5-9)

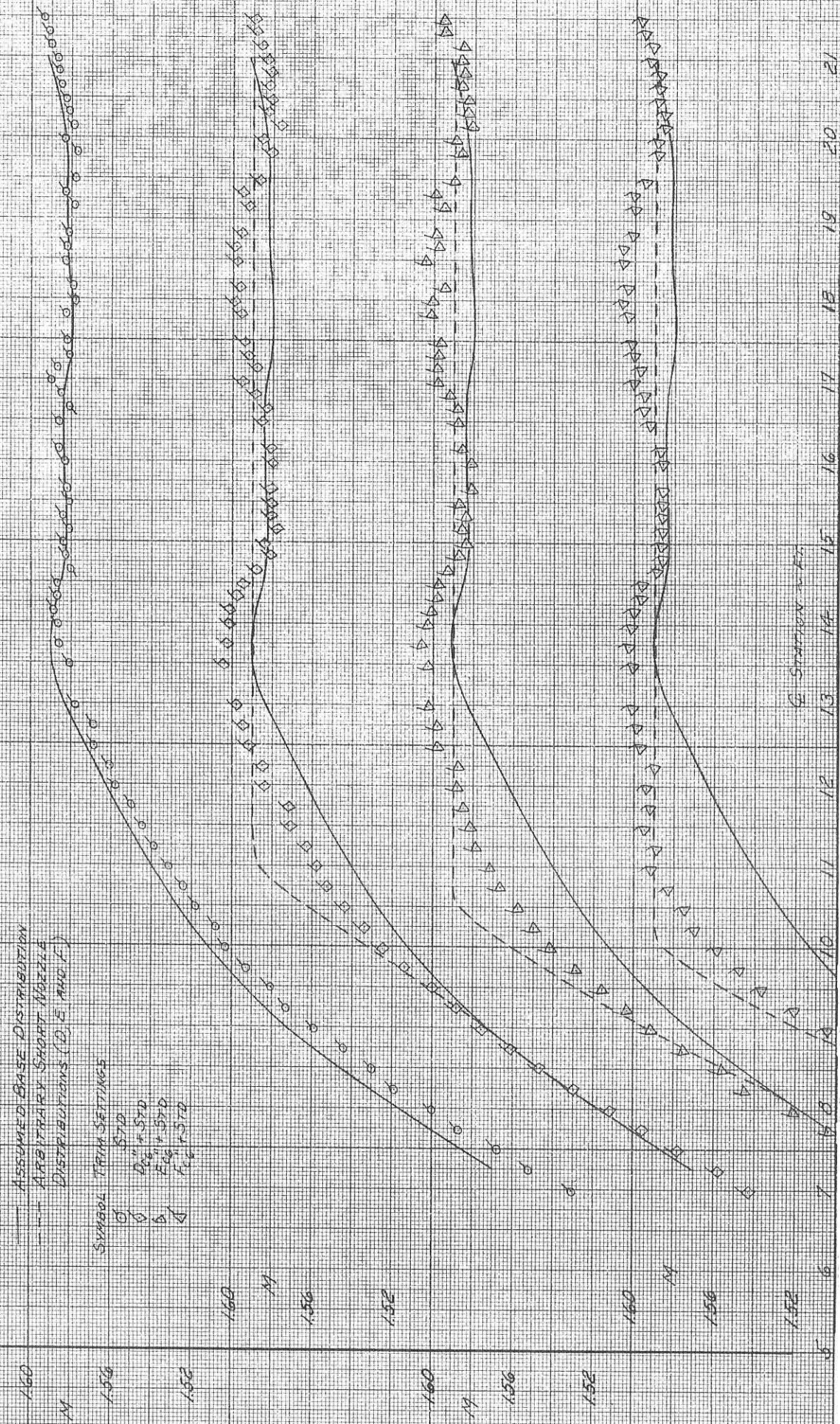
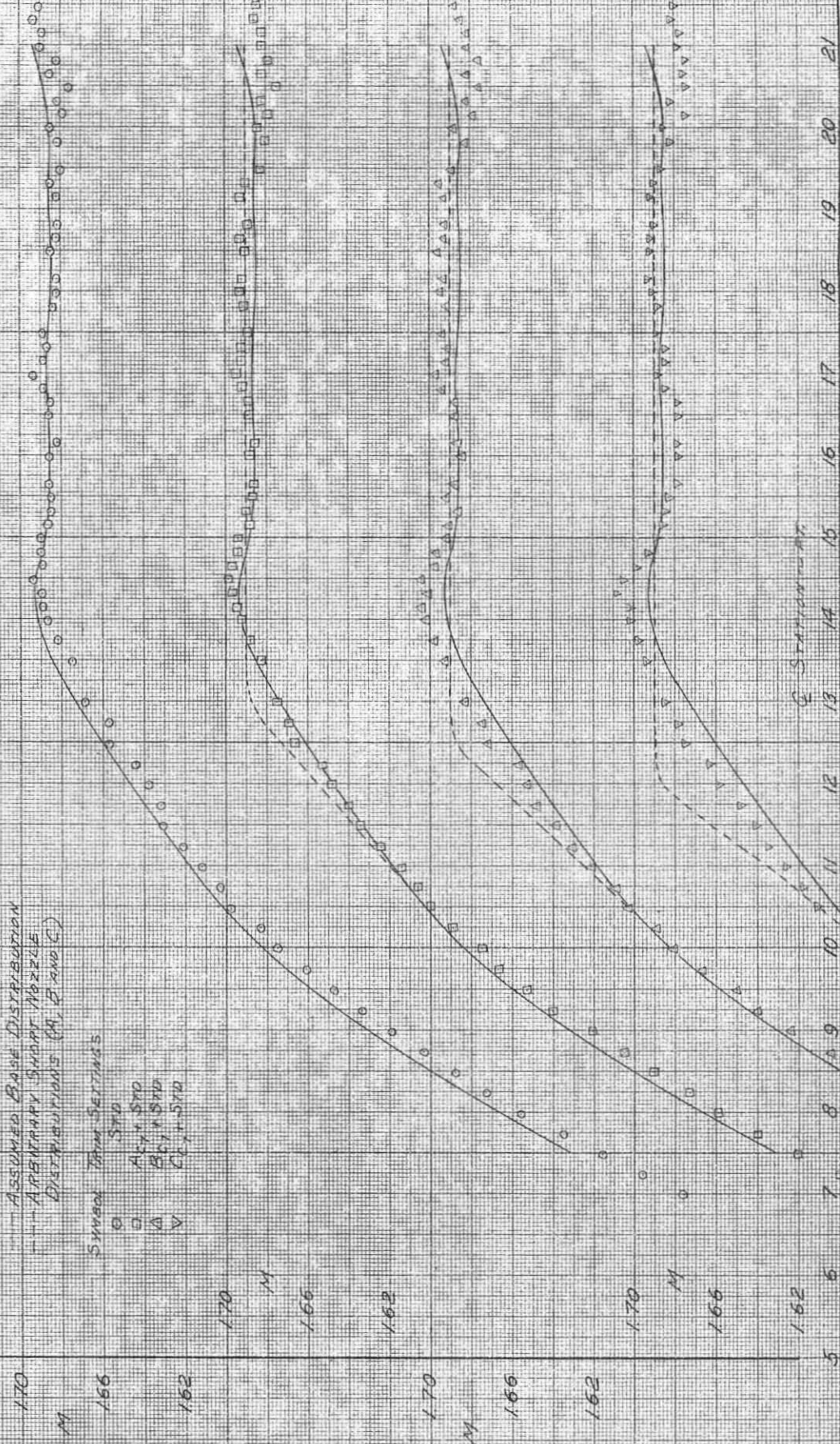


FIGURE 23. SHORT NOZZLE DISTRIBUTIONS A_C , B_C , AND C_C AT $M_{jet} = 1.00$ (AREAS 6-9)

ASSUMED BASE DISTRIBUTION
ARBITRARY SWIRL NOZZLE
DISTRIBUTIONS (M, E AND G)

SWIRL TRIM SETTINGS

- STD
- A_C STD
- △ B_C STD
- ▽ C_C STD



E Station No.

19 20 21

10 11 12

13 14 15

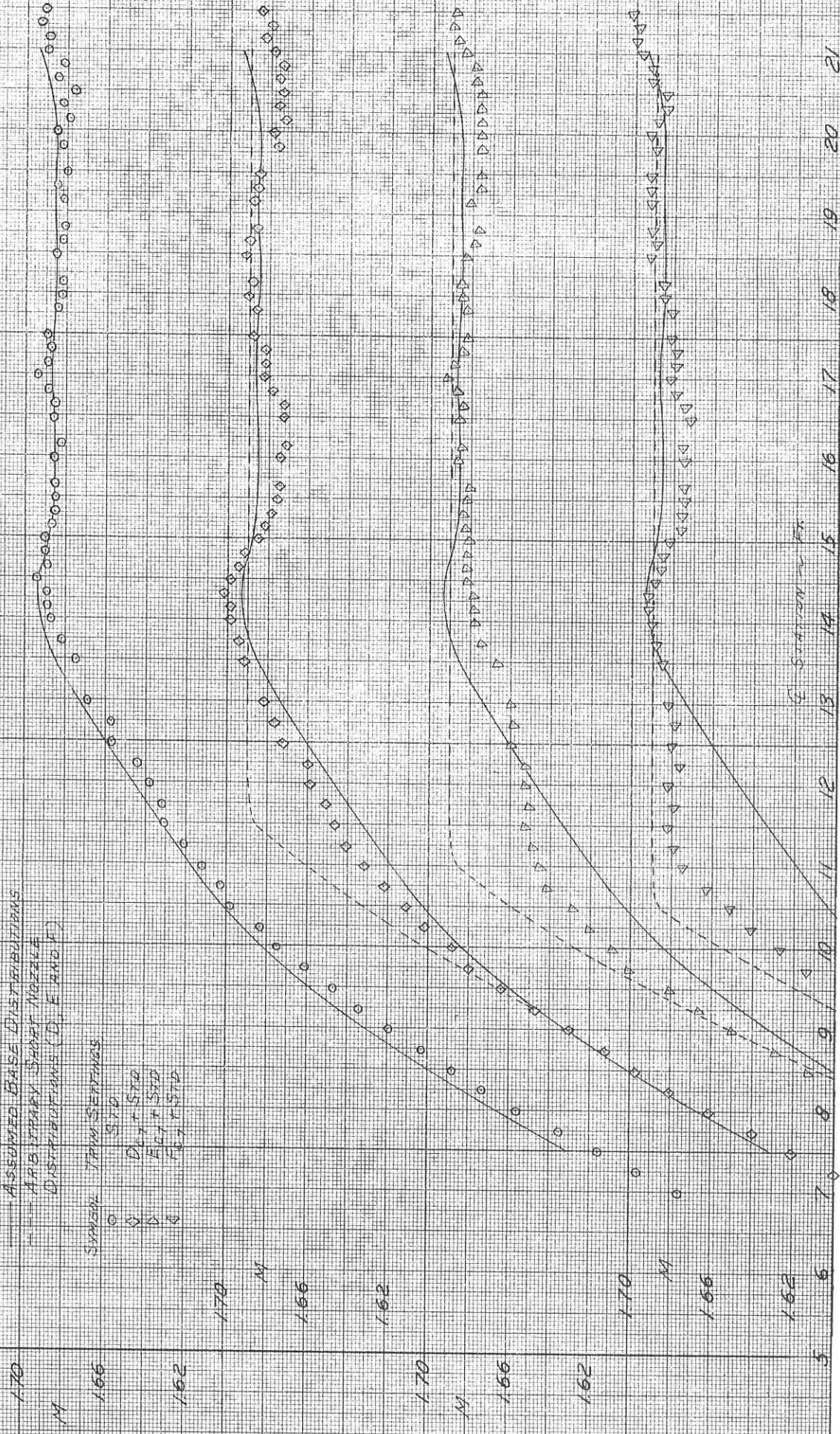
16 17 18

19 20 21

FIGURE 24 SHORT NOZZLE DISTRIBUTIONS D_{01} , E_{01} AND F_{01}
AT $M_{NOZ} = 1.00$ (CIRCS & D)

— ASSUMED BASE DISTRIBUTIONS
- - - ARBITRARY SHORT NOZZLE
DISTRIBUTIONS (D, E AND F)

SYMBOL TRIM SETTINGS
○ STD
◇ DELT STD
▽ FCT STD
◊ F₁ STD



STATION ~ X

FIGURE 25. SHORT NOZZLE DISTRIBUTIONS. D_{10}^* , E_{10}^* AND F_{10}^* AT $M_{NOZ} = 1.700$ (REFS 5-9)

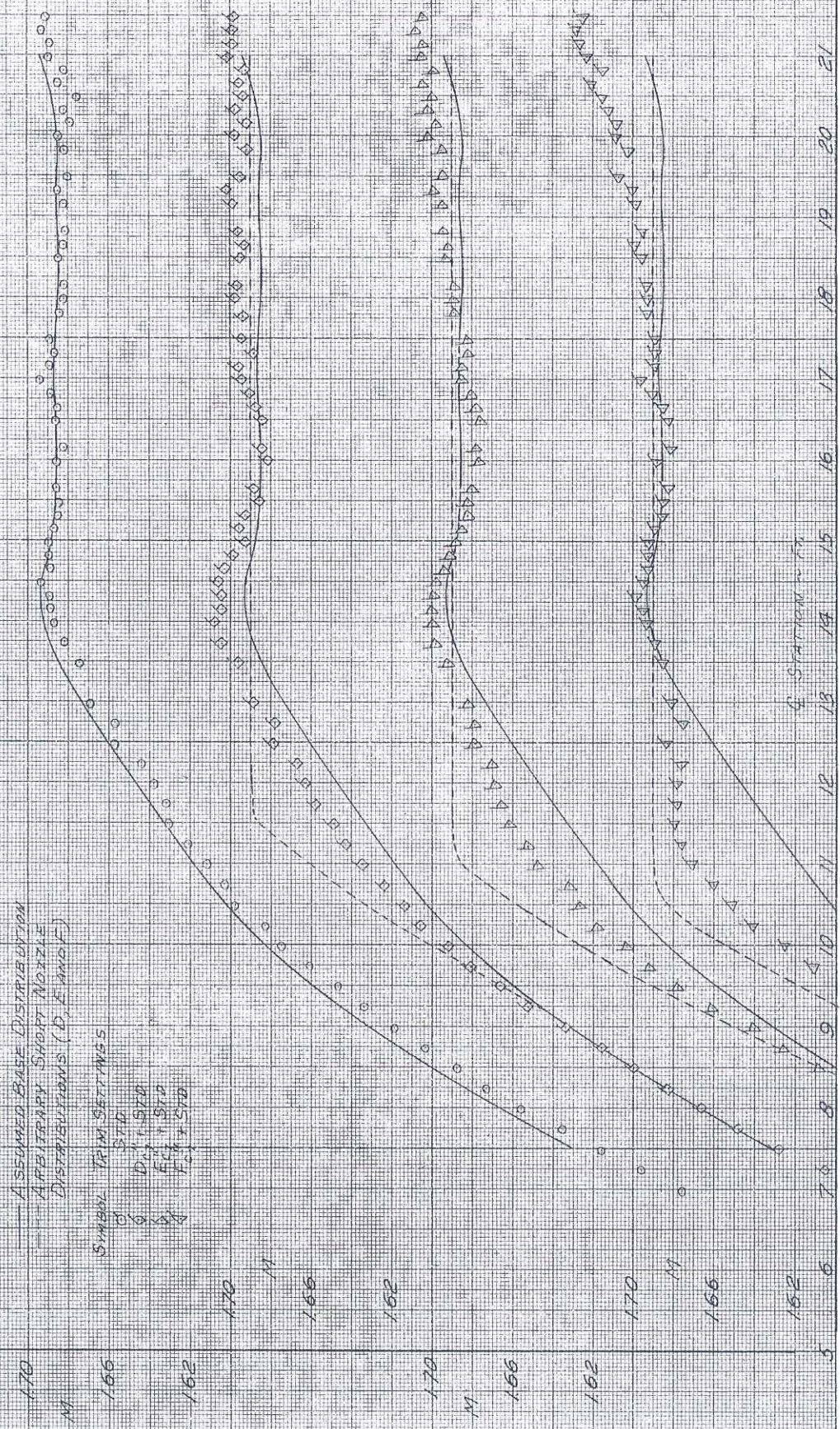


FIGURE 26. RELATIONSHIP OF ARBITRARY DISTRIBUTIONS AND SHORTEST THEORETICAL NOZZLES FOR $M_{1,AV} = 1600$ AND $M_{2,AV} = 1700$

